EMPIRICAL STUDIES OF CLOUD EFFECTS ON UV RADIATION: A REVIEW

Josep Calbó,[1] David Pagès, and Josep-Abel González[1]
Departament de Física, Universitat de Girona, Girona, Spain

Received 3 May 2004; revised 24 December 2004; accepted 19 April 2005; published 29 June 2005.

[1] The interest in solar ultraviolet (UV) radiation from the scientific community and the general population has risen significantly in recent years because of the link between increased UV levels at the Earth's surface and depletion of ozone in the stratosphere. As a consequence of recent research, UV radiation climatologies have been developed, and effects of some atmospheric constituents (such as ozone or aerosols) have been studied broadly. Correspondingly, there are well-established relationships between, for example, total ozone column and UV radiation levels at the Earth's surface. Effects of clouds, however, are not so well described, given the intrinsic difficulties in properly describing cloud characteristics. Nevertheless, the effect of clouds cannot be neglected, and the variability that clouds induce on UV radiation is particularly significant when short timescales are involved. In this review we show, summarize, and compare several works that deal with the effect of clouds on UV radiation. Specifically, works reviewed here approach the issue from the empirical point of view: Some relationship between measured UV radiation in cloudy conditions and cloud-related information is given in each work. Basically, there are two groups of methods: techniques that are based on observations of cloudiness (either from human observers or by using devices such as sky cameras) and techniques that use measurements of broadband solar radiation as a surrogate for cloud observations. Some techniques combine both types of information. Comparison of results from different works is addressed through using the cloud modification factor (CMF) defined as the ratio between measured UV radiation in a cloudy sky and calculated radiation for a cloudless sky. Typical CMF values for overcast skies range from 0.3 to 0.7, depending both on cloud type and characteristics. Despite this large dispersion of values corresponding to the same cloud cover, it is clear that the cloud effect on UV radiation is 15–45% lower than the cloud effect on total solar radiation. The cloud effect is usually a reducing effect, but a significant number of works report an enhancement effect (that is increased UV radiation levels at the surface) due to the presence of clouds. The review concludes with some recommendations for future studies aimed to further analyze the cloud effects on UV radiation.

Citation: Calbó, J., D. Pagès, and J.-A. González (2005), Empirical studies of cloud effects on UV radiation: A review, *Rev. Geophys.*, *43*, RG2002, doi:10.1029/2004RG000155.

1. INTRODUCTION

1.1. Description of UV Radiation: Related Radiative Magnitudes

[2] The Sun emits energy across the electromagnetic spectrum but mainly in wavelengths between 200 and 4000 nm. Energy emitted as function of wavelength is very similar to what is expected from a blackbody with a temperature near 6000 K, which is close to the Sun's photosphere temperature, while the averaged energy flux density emitted at the photosphere is 6.2×10^7 W m^{-2} [*Liou*, 1980], and the maximum emission, according to Wien's law, is found close to 500 nm. The distribution of radiation depending on wavelength (the so-called spectrum of emission) covers ranges (or bands) called visible (VIS) (between 400 and 720 nm), infrared (IR) (wavelength longer than 720 nm), and ultraviolet (UV). The ultraviolet radiation is defined as electromagnetic radiation having wavelengths within the range 200–400 nm, and it is divided into three different bands. UVC corresponds to wavelengths from 200 to 280 nm, UVB corresponds to wavelengths in the range from 280 to 315 nm, and UVA corresponds to wavelengths from 315 nm to the visible lower limit (400 nm). The boundary between UVB and UVA is somewhat ambiguous, and some authors set it at 320 nm, based on the significant biological effects of radiation with wavelength between 315 and 320 nm [e.g., *Webb*, 1998]. However, most international agencies and consortia agree in establishing this boundary at 315 nm: *World Health Organization* (*WHO*) [2002]; European Union's action COST 713 [*Vanicek et al.*, 2000]; *Commission Internationale de l'Eclairage* [1999]; and *International Agency for Research on Cancer* [1992]. According to *Frederick et al.* [1989], radiation in the UV band received at the top of the atmosphere is 8.3% of total solar radiation.

[3] When radiation emitted by the Sun (i.e., solar radiation) enters into the Earth's atmosphere, it is modified by several phenomena, which are classified into absorption and scattering (which together cause the beam extinction).

[1]Also at Institut de Medi Ambient, Universitat de Girona, Girona, Spain.

8755-1209/05/2004RG000155$15.00
Paper number 2004RG000155

One of the most important phenomena that influences UV radiation is the absorption by photochemical reactions, which, in general, are involved in the ozone creation-destruction cycle. These reactions, which take place basically in the stratosphere, virtually absorb all radiation in the UVC band. Even if stratospheric ozone were greatly reduced, all UVC would still be totally absorbed. However, radiation within the UVB and UVA bands is not totally absorbed in the stratosphere and reaches the Earth's surface in amounts that depend on tropospheric ozone content and the presence of other gases, aerosols, and clouds.

[4] Radiation flux density reaching a surface and coming from a single direction of the sky hemisphere is called radiance and has units of W m^{-2} sr^{-1}. Radiation reaching a flat surface and coming from a part of the sky hemisphere is called irradiance and has units of W m^{-2}. The irradiance from the whole sky hemisphere is called global irradiance, which is divided into direct and diffuse components. Direct irradiance is the beam of radiation coming from the Sun direction after extinction within the atmosphere, while the diffuse component is radiation coming from the whole sky hemisphere as result of scattering processes. Initially, when radiation coming from the Sun reaches the top of the atmosphere, there is only a direct component, but as it passes through the atmosphere, scattering processes redistribute this energy in other directions and increase the diffuse component at the expense of the direct component. All previous terms can be defined as monochromatic, i.e., for each wavelength, or panchromatic, i.e., integrated for all wavelengths. Also, these quantities can be defined for a range of wavelengths, e.g., UV diffuse irradiance or VIS radiance. We use the word broadband for panchromatic quantities in the shortwave range, i.e., solar radiation, which includes energy in the UV, VIS, and near IR bands.

[5] Since the effects of UV on live and inert materials depend strongly on wavelength, it is necessary to define the so-called action spectrum S(λ) [*Madronich*, 1993] in order to weight the importance of each wavelength on the development of each effect (e.g., damage to DNA, skin tanning, and material photodegradation). For example, UVB weights more than UVA in developing an erythema (reddening of the skin). In this case the action spectrum is the so-called erythematic function $S_{\mathrm{ery}}(\lambda)$, usually taken from *McKinlay and Diffey* [1987]. A spectral dose rate is the product of the irradiance reaching the Earth's surface $E(\lambda, t)$ and the action spectrum $S(\lambda)$. Moreover, we may define a dose rate $D_r(t)$ as the wavelength integration of the spectral dose rate:

$$D_r(t) = \int E(\lambda, t) S(\lambda) d\lambda. \tag{1}$$

Dose rates account for the energy that causes a specific effect. In particular, if the effect under study is erythema, dose rate is also called erythemal irradiance (E_{ery} or UVE). Finally, a dose is defined as the amount of weighted energy that may produce some effect and that reaches a surface during a specific time interval [*Madronich*, 1993]:

$$D(t_1, t_2) = \int_{t_1}^{t_2} D_r(t) dt. \tag{2}$$

Doses have units of J m^{-2} and can be defined for any period of time, although daily and annual doses are the most common.

[6] The so-called UV index (UVI) is a dimensionless quantity defined as 40 times the erythemal irradiance [*WHO*, 2002]:

$$\mathrm{UVI} = 40\mathrm{m}^2\mathrm{W}^{-1} E_{\mathrm{ery}} = 40\mathrm{m}^2\mathrm{W}^{-1} \int_{\lambda=250\mathrm{nm}}^{\lambda=400\mathrm{nm}} E(\lambda, t) S_{\mathrm{ery}}(\lambda) d\lambda. \tag{3}$$

Usually, the UVI is rounded off to the closest integer number and is calculated for the maximum erythemal irradiance in a day, but UVI has also been used to quantify any instantaneous or time-averaged UVE measurement. The UVI is intended as a simple measure of erythemal potential (or Sun burning power) for public dissemination.

[7] It is usual to consider the dose threshold above which the erythema begins to develop. This threshold is the so-called minimum erythemal dosage (MED) that depends on skin type (e.g., color and thickness). For a Caucasian population the definition of 1 MED can range from 200 to 450 J m^{-2} depending on skin type (Table 1). In order to avoid ambiguities the standard erythemal dosage (SED) has recently been defined as 100 J m^{-2} of erythemally weighted UV radiation.

[8] A sunburn time for each skin type can be defined as the maximum time to remain unprotected under the Sun without developing sunburns. Obviously, these times also depend on the UVE (or its equivalent UVI). For example, under a typical middle-latitude summer UVI value (about 8), 17 min of unprotected exposure is long enough to result in sunburn for a skin type I individual. Under the same conditions, 38 min would be required for a skin type IV individual to get minimal erythema.

1.2. Effects of UV Radiation

[9] The study of UV radiation reaching the ground is of great importance because of its interactions with biological material. When UV radiation reaches a cell or tissue, depending on wavelength, three different phenomena can occur: reemission, thermal dissipation, or absorption by chemical reactions. Specifically, absorption allows the formation of free radicals and reactive compounds that can produce effects in the organism in hours, days, or years. Some known effects are cell death, chromosome changes, mutations and morphologic transformation of cells, activation of genes and viruses (e.g., HIV), etc. [*International Programme on Chemical Safety* (*IPCS*), 1994].

[10] As far as UV interaction with humans is concerned, it is well established that UV is essential for human life,

TABLE 1. Definition of 1 Minimum Erythemal Dosage Depending on Skin Type[a]

Skin Type	Tan	Burn	Hair Color	Eye Color	1 MED,[b] J m^{-2}
I	never	always	red	blue	200
II	sometimes	sometimes	blond	blue/green	250
III	always	rarely	brown	gray/brown	350
IV	always	rarely	black	brown	450

[a]From *Vanicek et al.* [2000].
[b]MED is minimal erythemal dosage.

since it triggers the formation of vitamin D3 essential for building and maintaining bones [*Bryant*, 1997]. However, excessive UV radiation exposure may cause both acute and long-term harmful effects. Probably the most dangerous effect is the damage to DNA [*Diffey*, 1992] that has an action spectrum defined some time ago [*Setlow*, 1974]. This action spectrum has its maximum at 260 nm and almost no effect for wavelengths longer than 320 nm.

[11] Effects on human skin are well known and include immediate pigment darkening, i.e., the tanning caused by UVA that appears few hours after exposure; tanning caused by UVB that appears after some days; erythema that appears after 3–5 hours of exposition if the UVE dose has exceeded (by definition) 1 MED; nonmelanocytic carcinoma (including basal cell carcinoma and squamous cell carcinoma); and melanoma skin cancer (MSC) at the pigment cells [*Setlow et al.*, 1993]. Note that the first two effects are actually defense mechanisms against excessive UV exposure: A pigment (melanin) is produced in the epidermis in order to partially filter out UV radiation. According to *Repacholi* [2000], there are 200,000 cases of MSC every year worldwide, and if global ozone decreases by 10%, an increase of 4500 cases per year is foreseen because of the corresponding UV increase, although there is big uncertainty in the relationship between UV and MSC [*World Meteorological Organization* (*WMO*), 1994a]. The number of nonmelanocytic carcinoma cases is about 2 million per year worldwide; fortunately, this illness produces low mortality (1–2%). A decrease by 10% in global ozone may cause an increase of 0.3 million cases [*IPCS*, 1994].

[12] A third, and more common, effect on human beings is eye damage, which can occur mainly as cataracts or photokeratitis, both directly related with UV exposure. Although squinting is a partial natural defense against bright light (including sunlight with UV), it is accepted that eyes are quite vulnerable to UV exposures [*Vanicek et al.*, 2000]. In addition, eye damage is equally likely whatever the skin pigmentation (black, brown, or white). Eye damage is strongly related to UVA, since UVA penetrates deeper than UVB in the eye [*Bruls et al.*, 1984]. Cataracts are a deformation of the crystalline lens that can result in blindness. Some 20 million people worldwide are currently blind as a result of cataracts, and 20% of these cases may be related to excessive UV exposure [*WHO*, 1995]. A decrease by 1% of ozone column is estimated to produce 0.5% increase in new cataracts cases. Photokeratitis (snow blindness) is a transient blindness caused by inflammation of the cornea and iris that appears after an acute exposure to UV. Two hours in a place surrounded by snow covered surfaces can result in photokeratitis, while 6–8 hours are needed to develop it in a sandy area. Other less usual UV-related eye diseases are eye melanoma and photoconjunctivitis.

[13] Finally, some relations between UV and suppression of the immune system have also been reported [*WHO*, 1995; *Selgrade et al.*, 1997]. Suppression of the immune system triggered by UV exposure could lead to increased probability of developing herpes, increased susceptibility to certain infectious diseases, and decreased vaccine effectiveness, as well as the development of illnesses such as contact hypersensitivity response. More studies are needed to establish the role of UV in all these effects.

[14] Regarding UV interaction with aquatic and terrestrial ecosystems, the most dangerous effect is also damage to DNA, which may reduce photosynthetic activity, resulting in biomass and biodiversity losses. This is well documented for phytoplankton [*Neale et al.*, 1998; *Smith et al.*, 1992; *Sinha and Hader*, 2002]. In particular, *Prézelin et al.* [1994] estimates a 6–23% decrease of photosynthetic activity for Antarctic phytoplankton owing to ozone hole and subsequent ground UV rise. This effect has a clear link with climatic change since phytoplankton photosynthetic activity is an important CO_2 sink. Other effects can occur in phytoplankton such as decrease of movement capacity and indirect effects associated with food interactions [*Bothwell et al.*, 1994; *Hader*, 2000]. For example, damage to DNA can produce inhibition of some cell reactions, which may result in accumulation of some chemical species that can be transported to other organisms through the food chain.

[15] UV interaction with chemical compounds in the atmosphere is another particularly interesting field of research, since some reactions involved in photochemical smog need UV light to develop. The main factor here is the radiative flux available to a molecule (considered as an ideal point), which is called actinic flux by atmospheric scientists and spherical flux density by marine biologists. Direct measurements of actinic flux are notably difficult to perform. Therefore the actinic flux is usually estimated from irradiance measurements [e.g., *Webb et al.*, 2002; *Kylling et al.*, 2003]. Modeling actinic fluxes is important for pollution prevention, and while there are reliable models for cloudless conditions, simulation of actinic fluxes in cloudy skies is highly complicated because of the contribution of the diffuse component [*Van Weele*, 1996]. Recently, three-dimensional (3-D) radiative transfer models including clouds were developed for this purpose [*Brasseur et al.*, 2002].

1.3. UV Measurement Techniques

[16] There are different methodologies for measuring the UV radiation reaching the Earth's surface [*WMO*, 1999]. The first methodology uses ground-based instruments, which may be classified into four types. The first type of ground-based instruments developed for UV measurement are the so-called dosimeters [*IPCS*, 1994], which are devices that by nature respond directly to incident dose. Dosimeters may be modified further optically and calibrated to

respond according to an action spectrum, thereby serving as a direct-reading instrument for a dose that affects a particular receptor. These instruments are usually based on chemical species sensitive to UV. The second type is composed of radiometers, which can measure dose rates with a high sampling frequency. Erythemal biometers are a particular kind of these radiometers that have a spectral response close to the erythemal action spectrum. Erythemal biometers are often referred as Robertson-Berger sensors, after the pioneering instrument developed by Don Robertson and Daniel S. Berger [*Berger*, 1976], which was the first used extensively for monitoring purposes. These instruments, however, have some calibration problems that have not been completely solved. For this reason, *Weatherhead et al.* [1997] recommended they not be used in studies of long-time UVE trends. In general, it is accepted that their accuracy is within 10%. The third type, multichannel filter instruments, use different filters, allowing nearly simultaneous measurements at many wavelengths with resolution around 2–10 nm. These instruments allow the estimation of different types of dose rates since spectral information is obtained.

[17] Still among the ground-based instruments, high-resolution spectroradiometers constitute the fourth type. These devices can obtain the solar spectrum (in the UV and sometimes in the visible band too) with a typical spectral resolution of 0.5–1 nm but are much more expensive and need long scanning periods (some minutes). The advantage of spectral data is its versatility, while common problems that affect these kinds of measurements (and also the other instruments mentioned above) are calibration and angular deviation from the correct cosine behavior. Among these spectroradiometers a classical instrument is the so-called Brewer spectrophotometer, which was designed for ozone column measurement using ratios between irradiances at ozone absorbing and nonabsorbing wavelengths. In addition, Brewer instruments can measure calibrated (absolute) irradiances at any wavelengths between 286.5 and 363 nm in 0.5 nm steps. Other state-of-the-art spectroradiometers can measure with more extensive wavelength ranges. In general, interpolation and extrapolation procedures based on spectroradiometric measurements of monochromatic irradiances in the range between, say, 290 and 325 nm may lead to good estimation (uncertainties in the range 5–15%) of UV band irradiances such as UVE and UVI [*Webb*, 1998, 2000].

[18] The second methodology, and a very different approach for UV measurements, is satellite-based estimation techniques, which are built on radiative transfer models for the atmosphere together with measured reflectivities [*Ziemke et al.*, 2000; *Mayer et al.*, 1997]. The main difficulties with this technique are the effects of clouds and aerosols (particularly subpixel problems associated with broken and scattered clouds) and low spatial resolution or low frequency depending on the satellite orbit (geostationary or polar). All UV satellite-based estimations are based upon ozone measurement devices. The Total Ozone Mapping Spectrometer (TOMS) from NASA, currently on board the Earth Probe spacecraft, has provided estimations of ground erythemal UV since 1978. The Global Ozone Monitoring Experiment (GOME), operated by the European Space Agency (ESA), has also provided a global distribution of UV at the ground since 1995. Images from advanced very high resolution radiometer instruments on board NOAA satellites have been used to derive cloud characteristics for a better estimation of ground UV from GOME data [*Meerkoetter et al.*, 1997]. NOAA and the U.S. Environmental Protection Agency also forecast UV levels from ozone measurements made by TIROS Operational Vertical Sounder (TOVS) or solar backscattered ultraviolet/2 (SBUV/2) instruments on board NOAA polar-orbiting satellites, and new systems with improved products are being developed (e.g., Scanning Imaging Absorption Spectrometer for Atmospheric Chartography (SCHIAMACHY) from ESA [*Bovensmann et al.*, 2003]). Validation and cross comparison between ground-based measurements and satellite-based estimations is a very active area of current research, especially for the newest satellite sensors. *WMO* [2003] established that estimated UV radiation from TOMS is systematically higher than ground-based measurements, and for monthly averages, differences range between 0 and 40% for clean and polluted sites, respectively. However, when global- or regional-scale irradiances are to be analyzed, UV estimations from TOMS have so far been the most used.

1.4. Evidence of UV Increase at the Earth's Surface

[19] Large uncertainties are associated with the study of UV trends because of lack of both long-term databases and widespread, globally distributed measurements. In addition, the presence of masking phenomena such as cloud trends due to climate change and aerosol changes due to volcanic eruptions or anthropogenic sources add difficulties to UV trend detection. Moreover, UVB radiation can be absorbed by the increase in ozone that is occurring within the lower troposphere, especially around urban areas [*Bryant*, 1997]. However, good agreement is established in the connection between stratospheric ozone depletion and UV increase at ground level. Indeed, both models and measurements show UV increases corresponding to reduced ozone amounts [*WMO*, 1994a, 2003].

[20] Regarding the distribution of UV radiation at the Earth's surface, it is worth mentioning global UV climatologies, such as those developed by *Lubin et al.* [1998] using total ozone column (TOZ) from TOMS, water vapor from the International Satellite Cloud Climatology Project, reflectance from Earth Radiation Budget Experiment, and a radiative transfer code. They showed global distribution of UVB, UVA, UVB/UVA ratio, and TOZ. Regions with the maximum UVB are the tropics, high mountain areas such as the Andes, and low-cloudiness zones, mainly deserts, such as the Sahara. However, confirmation of these data from suitable ground-based measurements is still needed. A more recent UV climatology, highlighting the effect of aerosols on UV radiation, is the one presented by *Herman et al.* [1999].

TABLE 2. UVE Trends Given as Percentage per Decade by Latitudinal Bands

Latitude	Source		
	Herman et al. [1996][a]	*WMO* [1999][b]	*Ziemke et al.* [2000][c]
60°N	4.2 ± 3.7	3.7 ± 3.0	5.0 ± 5.5
40°N	3.0 ± 3.3	3.0 ± 2.8	3.9 ± 3.2
±30°	1.0 ± 3.0	0[d]	1.5 ± 3.0
40°S	2.5 ± 2.5	3.6 ± 2.0	2.5 ± 3.0
60°S	5.0 ± 4.7	9 ± 6	6.2 ± 4.5

[a]Values in this column are from Figure 2 of *Herman et al.* [1996]. The value for the ±30° band is a gross average of six bands in that image.
[b]Values are as they appear in the Executive Summary.
[c]Values in this column are from Figure 4 of *Ziemke et al.* [2000]. The value for the ±30° band is a gross average of 12 bands in that image.
[d]Trend is not statistically significant.

[21] Focusing on UV variations, the Executive Summary of the 1998 Scientific Assessment of Ozone Depletion [*WMO*, 1999] gives bulk trend estimations for several latitudes, corresponding to the period 1979–1992 and obtained from UV irradiances estimated from TOMS measurements but including cloud, aerosol, and albedo effects (see Table 2). In Table 2 the original published trends [*Herman et al.*, 1996], which are slightly different, are also shown. More recently, *Ziemke et al.* [2000] used almost the same database, but with a new cloud treatment, to derive new estimations of UVE trends. According to the latter authors the main differences between both analyses correspond to higher positive trends in UVE exposure at middle and high northern latitudes (Table 2). All these UV trends analyses, derived from satellite data, are restricted to latitudes between 65° south and north, because of limitations in obtaining reliable data at higher latitudes.

1.5. Factors Influencing Surface UV

[22] There are a number of factors that affect the amount of UV reaching a specific site at the Earth's surface. In this section we describe with some detail the most important, including some (e.g., ozone and latitude) that have already been mentioned above.

1.5.1. Astronomical Factors

[23] Astronomical factors refer to the position of the Sun relative to a specific site on the Earth. The most important factor influencing UV radiation reaching the ground is solar elevation (most commonly described through the solar zenith angle (SZA), i.e., the angle between the local zenith and the line of sight to the Sun) [*Schwander et al.*, 1997]. The higher the Sun from the horizon, the shorter the atmospheric path that radiation crosses before reaching the ground and the lower the extinction. Another astronomical factor is the variation of Earth-Sun distance due to elliptical orbit. As result of this variation the incoming solar irradiance varies by ±3.5% [*Iqbal*, 1983] throughout the year, and it is a maximum in December and a minimum in June. Another related factor is the solar activity, which has a well-established period of 11 years and is responsible for variations of 0.1% in the total solar energy output [*Lenoble*, 1993]. At short wavelengths, however, the latter effect may be larger (1.1% between 200 and 300 nm according *Lean et al.* [1993]).

1.5.2. Ozone

[24] Because UV (mainly UVC and UVB) is involved in ozone creation-destruction reactions, ozone concentration and vertical distribution have strong effects on the amount of UV reaching the ground. The anticorrelation between stratospheric ozone content and UV has been extensively demonstrated [e.g., *Kondratyev and Varotsos*, 2000] and already mentioned in section 1.4. The most important parameter describing ozone content is total ozone column, which is usually measured in Dobson units (DU), defined as the thickness (in 10^{-5} m) of the column at standard conditions of temperature and pressure, i.e., 1 atm and 273 K (1 DU = 2.69×10^{20} molecules m^{-2}). A radiation amplification factor (RAF) has been defined as the change induced in a UV radiation dose owing to a change in TOZ [*Madronich*, 1993]:

$$\frac{D_1}{D_0} = \left(\frac{\mathrm{TOZ}_1}{\mathrm{TOZ}_0}\right)^{-\mathrm{RAF}}, \tag{4}$$

where subindexes mean different conditions of ozone and radiation dose. For small TOZ changes the above expression can be linearized as

$$\frac{\Delta D}{D_0} = -\mathrm{RAF}\frac{\Delta \mathrm{TOZ}}{\mathrm{TOZ}_0}, \tag{5}$$

where Δ indicates the difference between values at the two different conditions. The RAF value for erythemal UV doses is around 1 [*Thomas and Stamnes*, 1999]; that is, a 10% decrease in TOZ turns out in a 10% increase in UVE.

[25] There is a well-known seasonal variation of TOZ: In both hemispheres, stratospheric ozone reaches higher concentrations in summer and autumn than in winter and spring. On the other hand, the most famous long-term and anthropogenic induced change of stratospheric ozone is the Antarctic "ozone hole," which is defined as the region with TOZ values less than 220 DU. Usually, the ozone hole reaches its maximum in spring, but in some years it also persists into early summer. In the last decade the ozone hole has increased in extension and deepened, therefore increasing the impact on UV doses at ground level. However, recent growth has not been as rapid as in the 1980s. In 2002 the ozone hole was one of the smallest ever observed and was divided into two parts because of particular meteorological conditions; however, the 2003 ozone hole was equal to the largest on record. Therefore it is not clear that the ozone layer has begun to recover [*WMO*, 2003]. Typical values of TOZ in winter/spring over Antarctica are 40–50% lower than the in pre–ozone hole period, reaching short (~1 week) episodes of 70% reduction. Models predict that Antarctic ozone levels will be increasing by 2010 and return to pre-1980 levels by the middle of this century [*WMO*, 2003]. This recovery is likely a result of the Montreal Protocol in 1987 and its subsequent amendments and adjustments, which forces the parties to phase out the

TABLE 3. Ozone Depletion Facts[a]

Region	Ranges of TOZ,[b] DU		Ozone Trends,[c] Percentage per Decade ±2σ		
	1964–1976	1985–1997	Annual	December–May[d]	June–November[e]
Arctic (~65°N)[f]	275–475	275–425	−5.7 ± 1.6	−7.8 ± 2.7	−3.5 ± 1.5
50°–65°N	300–425	275–400	−3.7 ± 1.6	−4.4 ± 2.6	−2.8 ± 1.3
30°–50° N	300–425	275–400	−2.8 ± 1.7	−3.8 ± 2.4	−1.7 ± 1.3
Equator ±20°	250–275	250–275	−0.5 ± 1.3	−0.3 ± 1.6	−0.7 ± 1.3
30°–50° S	300–375	275–350	−1.9 ± 1.3	−2.4 ± 1.2	−1.4 ± 1.9
50°–65° S	300–375	275–350	−4.4 ± 1.8	−3.4 ± 1.6	−5.2 ± 2.6
Antarctic (~75°S)[f,g]	275–350	175–300	−8.9 ± 2.0	−6.3 ± 1.9, −2.4 ± 3.2	−6.5 ± 4.3, −20.0 ± 4.0

[a]Table 3 is from *WMO* [1999].
[b]Ranges are from mean monthly values obtained at ground stations.
[c]Ozone trends are from Total Ozone Mapping Spectrometer.
[d]This corresponds to winter/spring in the Northern Hemisphere and to summer/fall in the Southern Hemisphere.
[e]This corresponds to summer/fall in the Northern Hemisphere and to winter/spring in the Southern Hemisphere.
[f]Polar trends are not from TOMS measurements but are from ground stations.
[g]For Antarctica we provide four trends, corresponding to the four seasons, in order to make apparent the large depletion in spring months (i.e., ozone hole).

emission of ozone-depleting substances such as chlorofluorocarbons (CFC), hydrofluorocarbons (HCFC), and methyl bromide. Although a substantial reduction of emissions has already been achieved and concentrations of depleting substances have been reduced in the troposphere, concentrations of almost all these species are still increasing in the stratosphere.

[26] Table 3 summarizes the most relevant facts regarding ozone depletion. Typical TOZ levels derived from ground stations for several latitudinal bands before (1964–1976) and after (1985–1997) the beginning of ozone depletion and trends in ozone content derived from satellite measurements (TOMS) between 1979 and 1997 are shown. Ozone depletion has also been observed in and around the Arctic pole, reaching maximum reductions of 30% during the last decade. This reduction is lower and more variable than in Antarctica because of the lack of a strong polar vortex (a cold air region in the stratosphere, isolated by a stream of strong winds circulating around the edge of this region). Indeed, geographic symmetry about the North Pole is less than about the South Pole. This fact makes the Arctic polar vortex less stable than the southern equivalent. As a result, temperatures are never as cold in the Arctic as they are over Antarctica, and fewer polar stratospheric clouds (PSC) are formed in the Arctic. Note that the presence of PSC is a key factor in promoting production of chemically active (i.e., ozone depleting) chlorine and bromine [*WMO*, 1999]. Models predict that maximum ozone depletion in the Arctic will be reached in the next 2 decades but never with values as low as in Antarctica. As far as other latitudes are concerned, in midlatitude regions of the Northern Hemisphere depletion is higher in winter/spring than in summer/fall, with an average reduction of 3%. Differently, at midlatitudes of the Southern Hemisphere the ozone reduction is less variable throughout the year.

[27] Ozone is not exclusive to the stratosphere. Ozone is also found in the troposphere because of a series of photochemical and chemical reactions that involve UV light, nitrogen oxides (NO_x), and volatile organic compounds (VOC). While ozone in the stratosphere is beneficial for human life, acting as a filter for UV, ozone in the lower troposphere is considered a pollutant since its high oxidant capacity causes several adverse reactions, such as irritation, respiratory problems, or degradation of materials. Tropospheric ozone tends to increase as a result of increasing emissions of its precursors (NO_x and VOC), mainly in urban areas, and of increased UV (linked to stratospheric ozone depletion). Because tropospheric ozone production depends on the presence of its precursors, its distribution is highly inhomogeneous: Peak concentrations are found in industrialized countries despite the strong regulations to control hazardous levels. Despite this nonuniform distribution, *Seinfeld and Pandis* [1997] set a typical value of 30 DU as a global average of tropospheric ozone content.

[28] Tropospheric ozone is also highly variable in time, both seasonal and daily scales. Owing to the photochemical mechanisms that synthesize ozone, minimum ozone concentration is usually found early in the morning, while the maximum value is set in late afternoon. Changes in tropospheric ozone from day to day can be as large as a factor of 2 or 3. Regarding long-time trends, the *WMO* [1994b] estimates an enhancement of boundary layer ozone levels of up to 50% in some populated Northern Hemisphere regions; *Janach* [1989] estimates a global averaged increase of 1–2% for tropospheric ozone between the 1960s and 1989; and the *Intergovernmental Panel on Climate Change* [2001] assigns a small but significant positive radiative forcing to increased tropospheric ozone concentration, which is estimated to be some 8 DU between 1750 and current days. Although tropospheric ozone is very variable both in time and space, it has been suggested that in industrial areas of the Northern Hemisphere increased tropospheric ozone can overcompensate (as far as filtering UVB is concerned) for stratospheric ozone depletion [*Brühl and Crutzen*, 1989].

1.5.3. Clouds

[29] Because clouds are formed by small water droplets or ice crystals, radiation is scattered when passing through

them, resulting (in general) in extinction or diminished transmissivity of the atmosphere. Clouds are highly variable in time and space, so there is great difficulty in their specification, and their usual effect is attenuation of surface UV [*Bais et al.*, 1993]. More specifically, *Frederick and Snell* [1990] found mean annual cloud attenuations between 22 and 38% at several sites in the United States; *McKenzie et al.* [1991, 1996] reported attenuation due to clouds of 25–30% in the global UV reaching the ground; *Lubin et al.* [1998] found attenuation of 10–25% in the rain forest; and *Estupiñán et al.* [1996] noted that attenuation may be undetectable for very thin clouds or small cloud amount but may be as high as 99% under extremely thick clouds. Moreover, *Ziemke et al.* [1998] stressed the importance of cloud effects in day-to-day variability of UV levels at the surface. Attenuation depends on different cloud properties such as cloud amount, cloud optical thickness, relative position between the Sun and clouds, cloud type, number of cloud layers, etc. Ground level UV radiation may be affected by clouds in such a manner that sometimes it may be higher than UV radiation in cloudless conditions. This effect, known as cloud enhancement, is described in various studies [*Estupiñán et al.*, 1996; *Schafer et al.*, 1996; *Sabburg and Wong*, 2000a; *Sabburg et al.*, 2003], but the magnitude of this enhancement is not well established. Since cloud effects on UV radiation are precisely the focus of the present paper, detailed quantification of cloud influences on UV will be addressed extensively later.

1.5.4. Aerosols

[30] Particles suspended within the atmosphere cause extinction of radiation because of scattering and absorption. Particles are highly variable in their chemical and physical properties (composition, size, or degree of aggregation) both in time and space, but some systematic treatments and modeling have been developed in order to describe their optical properties on a physical basis [*D'Almeida et al.*, 1991; *Koepke et al.*, 1997; *Hess et al.*, 1998]. Effects of aerosols on UV radiation are more noticeable in regions that are next to sources of dust and smoke [*WMO*, 1999]. *Krzyscin and Puchalski* [1998] stated that the daily variation of aerosol optical depth may be responsible for changes of up to 20–30% in UVE. *Erlick and Frederick* [1998] studied, by modeling, the aerosol effect relative to an aerosol-free atmosphere. They found a reduction in transmission of 15.2% for continental aerosol and 40.0% for urban aerosol, both at 310 nm and assuming average summer humidity conditions. These reductions correspond to predicted aerosol optical depths (AOD) at 310 nm of 1.26 and 3.22, respectively. *Seckmeyer* [2000] studied the reduction of transmission due to AOD; he obtained a reduction of 20% at 355 nm when AOD is increased from 0.1 to 1. *Estupiñán et al.* [1996] found, for North Carolina (United States) and using 6 months of ground-based data, reductions in the range of 5–23% on hazy days, compared to clean and dry conditions. *Krotkov et al.* [1998], on the basis of TOMS data, found that aerosol absorption can produce a very large reduction (~50%) in UV flux in certain parts of the world (e.g., those affected by forest fires or blowing desert dust).

1.5.5. Albedo

[31] Albedo is the ratio between the shortwave irradiance reflected from a system and the incident irradiance on the system. Both local albedo (the albedo of the nearest surfaces up to some hundred meters) and regional albedo (including surfaces up to 10 km distance) have some influence on UV incoming radiation [*Madronich*, 1993]. Albedo has strong wavelength dependence; in the UV band, albedo for most surfaces is below 0.1, quite lower than albedo in the visible band. When albedo is low and the sky is cloudless, an uncertainty of 1% in its value results in uncertainties of estimated UV irradiances of less than 0.5%. However, there are some very specific surfaces with higher UV albedo: sand (~0.25) and snow (~0.90). Nevertheless, snow albedo is highly dependent on the type and age of the snow [*Vanicek et al.*, 2000; *Kalliskota et al.*, 2000]. When covered with snow, surfaces surrounding a site can significantly affect UV irradiances [*Weihs et al.*, 2000]. *Renaud et al.* [2000] reported enhancements in UVE measurements on a snow-covered surface (with respect to the same, but snow-free, surface) of 15–25% under cloudless skies and up to 80% under overcast sky.

1.5.6. Altitude

[32] The higher above sea level, the shorter the optical path that solar radiation has to cross to reach the surface and, obviously, the lower the extinction suffered. The altitude effect is often evaluated by a single value, despite its dependence on wavelength and SZA [*McKenzie et al.*, 2001]. For cloudless sky, UVB increases of 2–23% km^{-1} [*Bener*, 1972; *Blumthaler*, 1993; *Piazena*, 1996], UVA increases of 7–15% km^{-1} [*Piazena*, 1996], increases of 6–18% km^{-1} for UVE [*Frederick et al.*, 1993; *Blumthaler et al.*, 1992, 1994a], and increases of 6–8% km^{-1} for UVI [*Vanicek et al.*, 2000] have been reported.

1.5.7. Relative Importance of Relevant Effects

[33] The relative effect of the several factors introduced in sections 1.5.1–1.5.6 depends on the timescale concerned. For example, *Bernhard et al.* [1997] showed that variability of UVE daily dose in a specific site may be typically around 24%, of which TOZ variability explains only 3% and the rest comes from cloudiness. Accordingly, *Krzyscin and Sobolewski* [2001] affirmed that the main UVE day-to-day variability is induced by clouds and aerosol but not by TOZ. Also, *Lubin et al.* [1998] showed that main variability of UV in otherwise homogeneous regions comes from cloudiness. Regarding longer timescales, *Bais et al.* [1996] pointed out that the effect of clouds on UVE variability is almost the same as the variability induced by seasonal changes in TOZ. Similarly, *Madronich* [1993] concluded that clouds are one of the major uncertainties in estimation and forecasting of UV trends, since their daily, seasonal, or long-term variability can hide UV trends due to ozone depletion. There is a broad agreement therefore in that (1) clouds are probably the factor that introduces most uncertainty when describing UV flux variability both at short and long timescales and (2) the effects of clouds are quite complex and depend on cloud characteristics (usually

unknown or only partially known) as well as other factors such as surface albedo and atmospheric aerosol content.

1.6. Methods for Studying Cloud Effects on UV Radiation

[34] The methodologies that have been used so far for analyzing cloud effects on attenuating or enhancing UV radiation at the surface are diverse, depending on both the approach taken (theoretical or empirical) and the goal of the analyses (climatology, forecasting, biological effect, etc.)

[35] Theoretical approaches include use and development of radiative transfer theory accounting for the effect of cloud particles (droplets or ice crystals) on UV. Great uncertainties still exist, particularly regarding ice clouds, mainly because application of Mie theory is very difficult with nonspherical particles such as ice crystals [*Liou*, 1992]. The most important physical variables that describe water clouds are droplet-size distribution and density (or, alternatively, optical thickness and effective radius). If there is more than one phase (i.e., water and ice), we need these two variables for each phase plus the corresponding mixing ratios. Several widely used plane-parallel radiative transfer models (i.e., 1-D models that consider the atmosphere as a series of horizontal layers with homogeneous characteristics) include cloud treatment and can be used as a first approach to analyze UV behavior under cloudy conditions [e.g., *Forster*, 1995]. However, cloud spatial variability makes the radiance field more complex than that simulated by plane-parallel models. Therefore the effect of nonhomogeneities suggests the need to use more complex views, such as 3-D models. These complex models are currently used in short-timescale studies of, for example, cumulus episodes, while simple 1-D codes are still used in climatic studies and in monitoring applications. The reason for this is that 3-D models need much higher computational power and more comprehensive input information, and they are impracticable in extensive modeling.

[36] Empirical approaches are often used to deepen our understanding and extend the characterization of cloud effects on UV radiation. In general, empirical studies use some method to simulate cloudless radiation and identify cloud effect as the difference between measured radiation (in cloudy conditions) and the estimated cloudless value. These approaches do not need as many input data as theoretical ones, but still, some of the required variables are difficult to measure. In particular, aerosol load and characteristics and total ozone column may be needed for the cloudless sky estimation. Empirical approaches focus on the study of macroscopic effects, and relations with cloud microphysics are quite difficult to establish. From these methods, cloud effects are computed as the part of the measured radiation that cannot be explained by the cloudless model, therefore missing distinction between different attenuation factors and enhancing phenomena that might occur simultaneously. Variables involved in these methods are cloud amount (either as cloud cover or as sky condition: clear, scattered, broken, and overcast), relative position between clouds and Sun (e.g., Sun obscured or not), and other variables such as solar broadband irradiance. Cloud cover is typically recorded in oktas (i.e., eighths of sky), tenths, or fractions of 1. Different studies choose different variables depending on their availability. Empirical studies of cloud effects on UV radiation are the focus of the present paper and will be reviewed in detail in section 2.

2. EMPIRICALLY DERIVED CLOUD EFFECTS ON UV RADIATION

[37] Most methods reviewed below study the ratio between measured UV irradiance in cloudy skies and an estimated cloudless UV irradiance. Instead of irradiance, sometimes dose is used. We will adopt for this ratio the expression cloud modification factor (CMF). Therefore

$$\mathrm{CMF} = \frac{\mathrm{UV}_m}{\mathrm{UV}_{\mathrm{cl}}}, \tag{6}$$

where UV_m is the actual measurement of the UV-related quantity and $\mathrm{UV}_{\mathrm{cl}}$ is the estimate of the same quantity in a cloudless sky but considering that all other conditions are kept the same as in the actual measurement. Usually, UV quantities are erythemal weighted irradiances, but sometimes they might be nonweighted UV values. CMF, depending on each particular study, may be given as a function of cloud cover, cloud cover and type, broadband (total) solar irradiance, and so on. Also, depending on the study, CMF values may be given as a graphical representation, as tabulated values, or (more usually) as an analytical function.

[38] Some characteristics of each reviewed work, including UV magnitude considered, instrument used for measurements, site(s), length of database, and some results, are summarized in Table 4. In sections 2.1–2.5 the most important methodological aspects and the main findings of each work are described, while further comparison among different techniques and results, and the corresponding comments, are left to section 3.

2.1. Methods Based on Visual Observations of Cloud Amounts

[39] Many of the pioneering studies of cloud effects on UV radiation were based on visual observations of clouds (e.g., *Buttner* [1938], as discussed by *Johnson et al.* [1976], and *Bener* [1964]). Probably, the reason for that was the availability of such kind of cloud data. One of these first works, by *Paltridge and Barton* [1978], was developed within the framework of the first erythemal UV climatology for Australia, and its results have been used by the operational Australian UVI forecast [*Lemus-Deschamps et al.*, 1999]. *Paltridge and Barton* [1978] pointed out the subjective nature of human observations of cloudiness but stressed that monthly statistics, which are used to build the UV climatology, are accurate enough. Cloudless dose was estimated from the envelope of the maximum readings in the plot of erythemal daily doses as a function of time throughout the year. According to *Paltridge and Barton* [1978], the effect of clouds is the result of two phenomena:

TABLE 4. Summary of Several Characteristics and Results of the Reviewed Works[a]

Source	Studied Variable	UV Instrument	Time Basis	Measurement Sites	Length of Database	CMF for Overcast Sky	Enhancement Effect	Fitted Formula/Comments
				Methods Based on Visual Observations of Cloud Amounts				
Paltridge and Barton [1978]	erythemal UV dose	Robertson-Berger sensor	day	one site, Australia	1 year	0.2	observed	see Figure 1
Josefsson [1986]	UV damaging dose	Brewer spectroradiometer	day	several sites, Sweden	60 samples	0.3	observed	$CMF = 1 - 0.7\left(\frac{N_d}{24}\right)^{2.5}$, N_d means total daily cloud cover
Ilyas [1987]	UV (295–390 nm)	Eppley UV sensor	month	Penang, Malaysia	4 years	0.44		$CMF = 1 - 0.056\,C$
Lubin and Frederick [1991]	irradiance at 345 nm (342.5–347.5 nm)	spectroradiometer	instant	Antarctic Peninsula	700 samples (spring)	0.54 (low clouds plus snowfall, 0.432; thin middle clouds, 0.845)	observed	$CMF = 1 - 0.0024C - 0.0038C^2$
Bais et al. [1993]	spectral UVB but mean CMF for the UV band given	Brewer spectroradiometer	instant	Thessaloniki, Greece	several years, SZA = 50°, TOZ = 315–341 DU	0.2	observed	$CMF = 1 + 0.06N - 0.02N^2$ ($3 \leq N$), $CMF = 1$ ($N \leq 3$), see Figure 2
Burrows [1997]	UVI	Brewer spectroradiometer	instant	Toronto, Canada, checked portability at 11 Canadian sites	4 years SZA < 70°, LST = 1000–1400	<0.4	observed and predicted	see Figure 3
Long et al. [1996]	UVI	Robertson-Berger sensor and Brewer spectroradiometer	hour	nine sites in United States	1 year plus 2 years for testing, samples at solar noon	0.316		see equation (7)
				Methods Based on Visual Observations of Cloud Amounts and Other Cloud Features				
Blumthaler et al. [1994b]	UVE and UVA (global and diffuse)	Robertson-Berger and Eppley UV sensors	10 min	Jungfraujoch, Switzerland (3576 m above sea level)	9000 records (16 periods of 6 weeks)	0.7 (high clouds, 0.9; middle clouds, 0.65) ratio CMF to CMF_{tot} up to 2	observed	see Figure 4
Thiel et al. [1997]	UVE	Robertson-Berger sensor	15 min	Garmisch-Partenkirchen, Germany	350 samples (spring and summer), SZA < 65°	0.28 (high clouds, 0.6; middle clouds, 0.31; low clouds, <0.25)	observed	$CMF = 1 - 0.71\left(\frac{N}{8}\right)^{2.85}$, see Figure 5
Frederick and Steele [1995]	UV (300–380 nm)	Eppley UV sensor	hour	Chicago, Illinois, USA	600 samples (not in winter)	0.55 (high clouds, 0.81; low clouds, 0.40) for noontime (i.e. lowest SZA)	observed	$CMF = 1.06 - 0.51f$
Kuchinke and Nunez [1999]	UVE	Robertson-Berger sensor (Solar Light 501A)	3 hours	Nordkoster Island (Sweden)	3 years (not in winter), SZA = 35°–70°	0.25	observed (particularly with cumulus and cirrus)	$CMF = 1 + 0.0266N - 0.0132N^2$ (SZA = 35°–59°), $CMF = 1 + 0.0065N - 0.0097N^2$ (SZA = 60°–69°)

TABLE 4. (continued)

Source	Studied Variable	UV Instrument	Time Basis	Measurement Sites	Length of Database	CMF for Overcast Sky	Enhancement Effect	Fitted Formula/Comments
Josefsson and Landelius [2000]	UVE	Robertson-Berger sensor	hour	Norköping, Sweden	10 years (35,000 samples) SZA = 5°–55°	0.35 (high clouds, 0.76)	observed	
Krzyscin et al. [2003]	UVE	Robertson-Berger sensor (Solar Light)	5 min	Belsk, Poland	2 years	0.58 (high clouds, 0.92; middle clouds, 0.63; low clouds, 0.53) ratio CMF to CMF_{tot} up to 1.8	observed (sometimes +20%)	$CMF = 0.02 + 1.65\ CMF_{tot} - 0.67\ CMF_{tot}^2$, see Figure 6
				Methods Based on Nonhuman Observations of Clouds				
Schafer et al. [1996]	UVB (290–320 nm)	Brewer spectroradiometer	instant	Black Mountain, North Carolina, USA	6 months (February–July) SZA = 30°–60°	0.296 (text and figures), 0.358 (fit)	observed (sometimes +11%)	$CMF = 1 - 0.1312C + 0.0287C^2 - 0.0022C^3$ ($4 \leq C \leq 10$), cirrus type clouds not included
Sabburg and Wong [2000b]	UVB	UVB sensor	6 min	Toowoomba, Australia	1 year	<0.3	observed	only samples with occulted Sun, cloud amount in part of the sky, many sky characteristics used
Grant and Heisler [2000]	UVB at 290 nm (258–315 nm)	International Light SED240 with UVB filter	10–20 min	West Lafayette, Indiana, USA	180 samples	0.65 CMF higher (factor 1.2) than CMF_{PAR}	observed	$CMF = 1.08 - 0.36f$
				Methods Based on Radiative Measurements Only[b]				
Bordewijk et al. [1995]	UV (285–345 nm, action spectrum for carcinogenesis in hairless albino mice)	spectroradiometer	instant, daily means	Bilthoven, Netherlands	several months SZA < 80°	<0.2 ratio CMF to CMF_{tot} up to 2	observed (+30%) and predicted	$CMF = 1.0(1 - e^{-2.7CMF_{tot}})$ (instantaneous) $CMF = 1.2(1 - e^{-1.8CMF_{tot}})$ (daily averages), see Figure 7
Bodeker and McKenzie [1996]	UVE	Robertson-Berger sensor	10 min	Lauder, New Zealand	1 year	ratio CMF to CMF_{tot} >2 at high SZA	observed	$CMF = A(SZA)CMF_{tot}^{P(SZA)}$ (for $CMF_{tot} \leq 1.0$), see Figure 8
Matthijsen et al. [2000]	erythemal UV dose	Robertson-Berger sensor	day	one site, Netherlands	6 months	ratio CMF to CMF_{tot} >1.5	observed and predicted	$CMF = 1.05\ CMF_{tot}^{0.84}$
Foyo-Moreno et al. [1999]	UV (290–385 nm)	Eppley UV sensor	hour	Granada and Almeria, Spain	2 years SZA < 80°	ratio UV/TOT irradiances from 3% to 6% (cloudy, low k_t cases)		$CMF = \frac{2.09\ W\ m^{-2}}{UV_{cl}} + 1.078\ k_t$
Nann and Riordan [1991]	spectral irradiance (320–1050 nm) on 48° south tilted surface	LICOR spectroradiometer	30 min (six scans)	Stuttgart, Germany	2000 samples (summer and fall) SZA < 72°	CMF at shortest wavelengths is 2 times CMF at 630 nm		

TABLE 4. (continued)

Source	Studied Variable	UV Instrument	Time Basis	Measurement Sites	Length of Database	CMF for Overcast Sky	Enhancement Effect	Fitted Formula/Comments
Methods Based on Both Radiative Measurements and Observations of Clouds[c]								
Estupiñán et al. [1996]	UVE	Robertson-Berger sensor (YES)	5 min	Research Triangle Park, North Carolina, USA	6 months (summer and fall) SZA < 70°	some cases with CMF <0.2	observed (up to +20%) and predicted	$CMF = 0.296 - 0.0279C + 1.72k_t + 0.000137C^2 + 0.0381Ck_t - 1.03k_t^2$
Schwander et al. [2002]	six wavelengths in the UV	Bentham spectroradiometer	instant	Garmisch-Partenkirchen, Germany, plus two sites for testing	2 years (10,000 samples) SZA = 25°–80°	some cases with CMF <0.2	observed (+20%) and predicted	only stationary conditions used, see Figure 9
Trepte and Winkler [2004]	UVE	Brewer spectroradiometer	hour	Hohenpeissenberg, Germany	9 years (March–October) SZA = 34°–70°	0.25 approximately	observed	$CMF = c_0 + c_1\,CMF_{tot} + c_2\,CMF_{tot}^2$ coefficients dependent on SZA, for samples when the Sun was obscured more than 5 min.

[a]Fitted formula is included if it can be written as function of cloud cover (either in oktas, N; in tenths, C; or in fraction of 1, f), as function of cloud modification factor for total solar radiation CMF_{tot}, or as function of clearness index k_t. Abbreviations are SZA, solar zenith angle; TOZ, total ozone column; and LST, local standard time.
[b]See *Krzyscin et al.* [2003] entries.
[c]See *Blumthaler et al.* [1994b] and *Grant and Heisler* [2000] entries.

backscattering and (small) direct absorption. Their results (see Figure 1) indicate that CMF is in the range between 1.0 (for 0 oktas, i.e., cloudless) and 0.2 (for overcast conditions). Individual points, however, show large scattering. For example, for 6 oktas, values of CMF extend over the range 0.5–0.9. Some effort was made by the authors to obtain CMF as function of cloud type or level. However, no statistically significant differences were observed between such curves. This is quite surprising since higher optical thickness usually associated with low-level clouds should result in larger attenuation than a corresponding amount of high-level clouds.

[40] A similar work was developed for UV damaging doses by *Josefsson* [1986], who proposed a simple parametric model in order to build a climatological representation of UV radiation in Sweden. In the model, all the relevant factors that affect UV radiation were considered: solar geometry, total ozone column, aerosol effect, albedo, altitude, and cloud effect (through accumulated daily cloud amount N_d). With the goal of finding an expression for the effect of clouds, CMF were plotted against N_d. Despite the large scatter of points (which *Josefsson* [1986] attributed to the imprecise description of clouds when using only three observations per day and without distinguishing cloud types), Josefsson suggested a continuous curve to fit the data (see Table 4). In addition, the points were grouped in three clusters, corresponding to three different day types:

Figure 1. Cloud modification factor (CMF), i.e., the ratio between daily measured erythemal irradiance (UVE) dose and estimated cloudless UVE dose, as function of cloud cover. From *Paltridge and Barton* [1978], reproduced with permission of CSIRO.

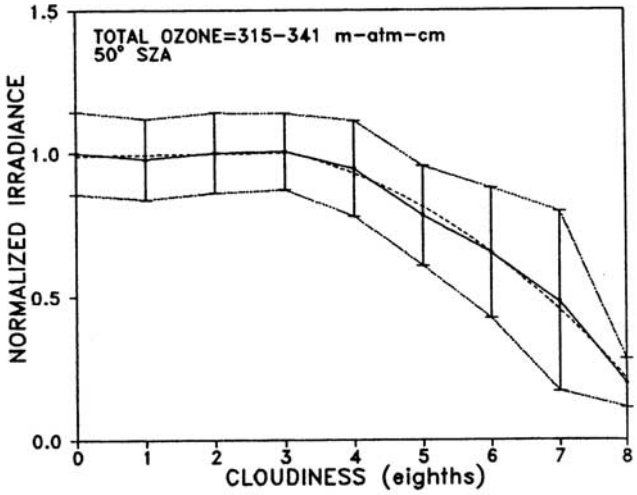

Figure 2. Mean (in the 290–325 nm band) CMF versus observed cloudiness (in oktas). For each cloud cover, dispersion of points is shown through ±1 standard deviation. The analytical fitted function is also plotted (dotted line). From *Bais et al.* [1993].

clear ($N_d \leq 6$ oktas), broken ($6 < N_d < 18$ oktas), and overcast ($N_d \geq 18$ oktas). For each day type the median of CMF values was evaluated: 0.98 for clear, 0.84 for broken, and 0.50 for overcast. There were also several points with CMF significantly larger than 1.0, i.e., what is called in later papers the cloud enhancement effect.

[41] One year later, in a short paper, *Ilyas* [1987] applied a simple relation originally suggested by *Buttner* [1938] to estimate monthly averages of UV radiation for Penang, Malaysia. Ilyas used this linear relation (see Table 4) along with the cloudless sky model by *Johnson et al.* [1976] and the monthly averages of cloud cover to obtain estimates of monthly UV radiation. He compared the results with measured values and obtained an overestimation in the yearly UV dosage of 7%, which is quite good if we consider the simplicity of the approach. *Ilyas* [1987] highlighted that even with very extensive cloudiness (e.g., 83% at his site, on average) the cloud effect is relatively low (reduces the influx by <50%). He pointed out, however, that the cloud effect on weighted irradiances might be different as a result of spectral dependence of cloud effect on UV radiation.

[42] *Lubin and Frederick* [1991] studied cloud effects on spectral UV radiation and analyzed their importance relative to UV increase because of ozone depletion in the Antarctic Peninsula. They stated that the year-to-year variability of seasonally averaged UV amounts is almost exclusively due to the degree of ozone depletion and is not affected by cloud cover, since the latter remains almost constant from year to year. However, cloud effects merit further investigation in shorter timescales, because the biological effects of UV may be affected by the high day-to-day cloud amount variability. Although they analyzed a narrow UV band (342.5–347.5 nm), cloud effects on UV were explicitly assumed to be spectrally independent, so results for this band could be useful for other UV wavelengths and for the UV band as a whole. For overcast conditions the obtained mean CMF was 0.54, which is higher than the corresponding values found in the previous works: 0.2 [*Paltridge and Barton*, 1978], 0.3 [*Josefsson*, 1986], and 0.44 [*Ilyas*, 1987]. The differences may be explained by different microphysical characteristics of polar clouds compared to midlatitude clouds, in particular, the lower optical depth of the former (at a site in the Antarctica, *Luccini et al.* [2003] also found CMF = 0.54 for clouds without precipitation). *Lubin and Frederick* [1991] summarized their results in a plot, and an analytical function (see Table 4) was fitted to the points. As usual, large scattering of individual values was reported: Averaged CMF for overcast with low clouds and snowfall is 0.432, while overcast with middle translucid clouds yields an averaged CMF of 0.845. In this work, more than 25% of cases had CMF greater than 1. These cases were found in all-sky conditions, and *Lubin and Frederick* [1991] hypothesized that light reflections in cloud edges may be the explanation of these enhancements.

[43] The work by *Bais et al.* [1993] was an attempt to establish the relative importance of variations in TOZ, SO_2 atmospheric concentrations, and cloud cover over spectral global UV irradiance reaching the ground. They showed that cloud effect on UV radiation has no spectral dependence, so it made sense to compute a mean CMF for the whole UV band. These mean CMF were plotted against cloud cover (see Figure 2), and an analytical expression was fitted to the values (see Table 4). No cloud effect was found, on average, for cloudiness up to 3 oktas, while the CMF was as low as 0.2 for overcast conditions. Enhancements (CMF > 1) were found for cloudiness as high as 4 oktas. Scattering of points is large, as is shown through error bars, and it is maximum for almost overcast conditions (6–7 oktas).

[44] Some studies have been developed as well with the goal of UV forecasting. For example, the system used by the Canadian Meteorological Centre is described by *Burrows* [1997]. In order to consider cloud effects with low computing cost the author investigated regression models among several variables typically supplied by weather forecasting models and the variable of interest, i.e., erythemal UV radiation. To build the appropriate regressions and check their ability, measured data (instead of forecasted data) were used. The normalized UV, defined as the actual UV divided by the cloudless sky UV (i.e., the CMF) was considered a dependent variable. The list of the independent variables (predictors) included both cloud observations (amount, type, altitude, etc.) and meteorological data (temperature, humidity, wind speed and direction, etc.) Two regression methodologies were tested: stepwise linear regression (SLR) and classification and regression trees (CART), which is a nonlinear regression technique. In the present review, we will comment only on CART results (which turned out to be better than SLR) that are based on cloud information. For practical purposes a regression with cloud cover, cloudless UV, and solar zenith angle as the only three predictors was checked. The error of this regression when applied to the original data was 35%. Burrows

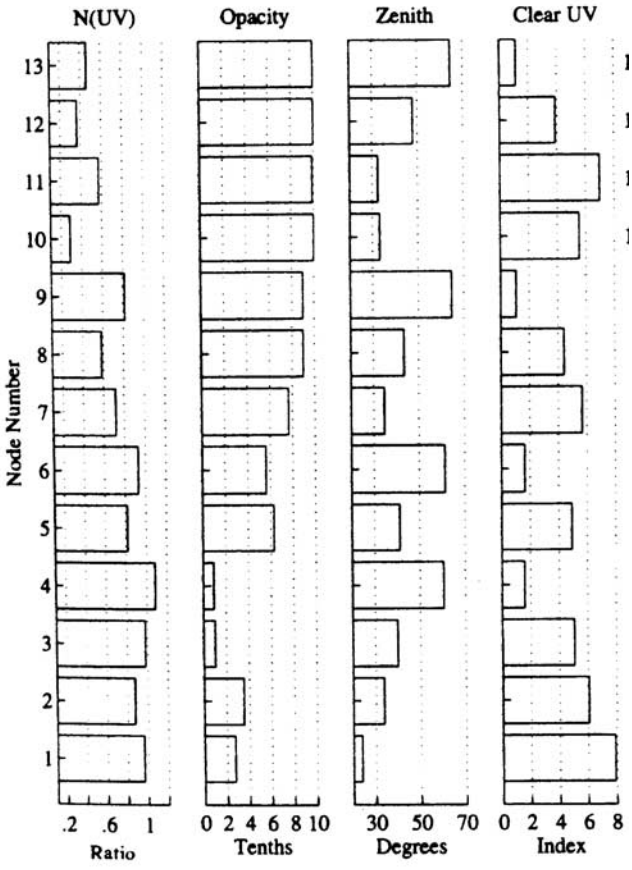

Figure 3. Means of variables in terminal nodes for the three predictors (opacity, i.e., cloud cover; solar zenith angle; and clear (cloudless) UV) for the database containing noon records with SZA < 70°. N(UV) is normalized UV, i.e., the cloud modification factor. From *Burrows* [1997], reproduced with permission of the American Meteorological Society.

claimed that, for forecasting purposes, the use of this simple regression would obtain better results than other options, which needed additional variables that bring their corresponding forecasting error. The prediction tree for this regression, which has 13 terminal nodes, was not reproduced in the original paper, but a figure was provided with the mean values of variables in each node (see Figure 3). One case (node number 4, low cloud cover, high solar zenith angle, low cloudless UV) may produce cloud enhancements, and two cases (node number 10 and node number 12) have CMF <0.4.

[45] Another technique for forecasting realistic (all-sky conditions) erythemal UV radiation had previously been reported by *Long et al.* [1996], where the method used by the U.S. National Weather Service and Environmental Protection Agency was described. Although the method is not based on actual observations of clouds, we have included it in this section because the analytical expression obtained relates cloud effect with cloud cover. Cloud-related information was the model output statistics (MOS) forecast probabilities for four sky conditions: clear (0–1 tenth), scattered (2–5 tenths), broken (6–8 tenths), and overcast (9–10 tenths). The simple correlation between UV observations (that allowed calculating CMF) and MOS probabilities of each sky condition is written in the following form:

$$\mathrm{CMF} = 0.316 + 0.676P_c + 0.580P_s + 0.410P_b, \qquad (7)$$

where c is for clear, s indicates scattered, b indicates broken, and P means probability for each sky condition. Therefore the CMF found for each sky condition were as follows: clear sky, 0.992; scattered clouds, 0.896; broken clouds, 0.726; and overcast conditions, 0.316. This regression was checked with data from 1993 and 1994, resulting in 76% of differences less than 1 UVI unit and in 91% less than 2 UVI units.

2.2. Methods Based on Visual Observations of Cloud Amounts and Other Cloud Features

[46] The works discussed in section 2.1 established relations between UV radiation reaching the ground and total cloud cover. Although *Paltridge and Barton* [1978] did not find different behavior for different cloud types, high dispersion in CMF for the same cloud cover and differences among averaged CMF for different climates (midlatitudes [*Bais et al.*, 1993], tropical [*Ilyas*, 1987], and polar [*Lubin and Frederick*, 1991]) seem to be related to different cloud types typically present at each site. In addition, although in the UV band a high proportion of the global radiation is in the diffuse component, obstruction of direct beam leads to a great decrease of radiation. Therefore some more recent studies attempt to include more sky condition characteristics in the study of cloud effects on UV. However, these extra cloud characteristics are difficult to know (e.g., optical thickness and drop size distribution are measured with high resolution only at specific sites and campaigns). So the most suitable possibility is the use of parameters observed more often, such as cloud amount, cloud type, or relative cloud-Sun position. These kinds of data usually show two problems: insufficient spatial and temporal coverage and the subjectivity of human observations [*Josefsson and Landelius*, 2000].

[47] For example, *Blumthaler et al.* [1994b] considered, besides total cloud cover, a classification of cloud types according to their altitude, distinguishing between cases when the Sun was obscured by clouds or not. For each magnitude (UVA, UVE, and broadband irradiances) both global and diffuse components were measured. Visual observations reported amount of cloudiness, cloud level (middle or high), and the screening of Sun by clouds (Sun free or totally covered) every 30 min. Some interesting conclusions can be extracted from the plots drawn in the original paper (see Figure 4). First, total global irradiance is more attenuated by clouds than UVE and UVA irradiances. This result was explained by spectral dependence of radiation scattering: Molecular (Rayleigh) scattering is more efficient for shorter wavelengths, resulting in a greater

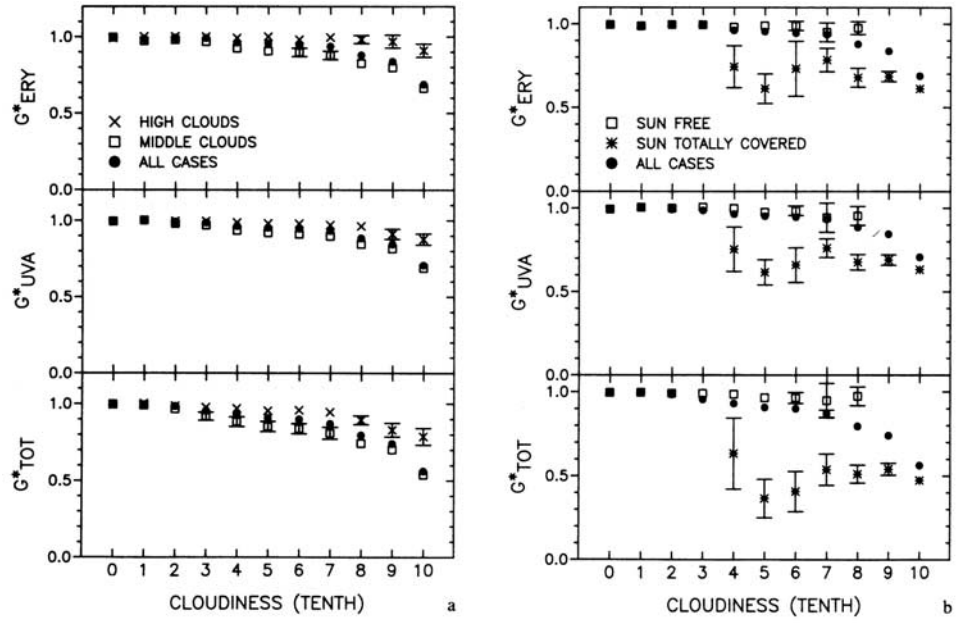

Figure 4. CMF (global normalized irradiance (G*) according to *Blumthaler et al.* [1994b]) versus cloudiness, averaged over all solar elevations depending on (a) cloud altitude and (b) screening of direct beam. Bars indicate ±3 standard error of the mean (which is quite small given the big number of experimental points used). ERY refers to erythemally active radiation; TOT refers to total solar radiation. From *Blumthaler et al.* [1994b], reproduced with permission of Springer-Verlag.

diffuse component in UV than in total solar radiation. In contrast, the cloud effect on UVE and UVA is quite similar, indicating little spectral dependence within the UV band. Second, for overcast conditions, mean CMF is 0.7 both for UVA and UVE. This very low reduction of UV radiation (lower than the 46% found by *Lubin and Frederick* [1991] in Antarctica) is explained by typically thin clouds at the site and high albedo of the surrounding surfaces (snowy environment). Third, the average CMF in overcast conditions produced by high clouds is 0.9, while the corresponding CMF for middle clouds is 0.65. Fourth, relative Sun-cloud position is a very important factor to be considered in cloud effect studies. For example, when total cloud cover is between 4 and 8 tenths, CMF is almost 1 if the Sun is not obscured, while it is around 0.7 when the Sun is obscured by clouds.

[48] The importance of cloud type in describing cloud effect on UV radiation is the focus of the paper by *Thiel et al.* [1997]. As other authors, they plotted CMF against total cloud cover and obtained minor cloud effects for $N < 5$ oktas and a large scatter of CMF values, particularly for N between 5 and 8 oktas. Despite the large scatter of values an analytical expression that relates CMF with cloud amount was adjusted (see Table 4). The fit was similar to that suggested by *Kasten and Czeplak* [1980] for total solar radiation and by *Josefsson* [1986] for UV radiation. The large scatter of CMF values was in part explained by the different cloud effect depending on the type of clouds present. Consequently, *Thiel et al.* [1997] aggregated their records in five categories: high clouds, altocumulus and altostratus (Ac/As), stratocumulus (Sc), cumulus (Cu), and cumulonimbus (Cb). Then, they fitted a similar function to each group of points and obtained values for the corresponding overcast CMF equal to 0.60, 0.31, 0.25, 0.12, and, 0 respectively (see Figure 5). It is clear that the higher the cloud liquid water content, liquid water path, or optical depth, the lower the CMF. The relationship between the coefficients of the fitted function and cloud physical characteristics was confirmed with data taken at the Zugspitze Mountain (2964 m above sea level), where higher CMF (indicating a higher transmissivity) was explained by the thinner clouds at high altitudes. On the other hand, several cloud enhancement cases were found for cases with $N < 7$ oktas; according to Thiel et al., uncertainties in estimating cloudless UVE and reflections in cloud edges may be the reasons for these enhancements.

[49] Instead of cloud type, *Frederick and Steele* [1995] included in their analysis cloud ceiling altitude and visibility. In a first instance, Frederick and Steele plotted CMF against fractional cloud cover and found the typical features of these kind of plots: a large dispersion of points and a low cloud effect for cloud fractions less than 6 tenths. They also found several cases of cloud enhancement effect. The large scatter of points was explained by a lack of information on cloud optical characteristics and also by differences depending on whether the Sun is occulted or not. In a second step, *Frederick and Steele* [1995] suggested and checked several regression models. A simple linear fit between CMF and cloud fraction (similar to that proposed by *Ilyas* [1987], see Table 4) explained 39% of the variance of CMF values. When information about the cloud ceiling altitude (which is clearly related to cloud type) was added, the corresponding

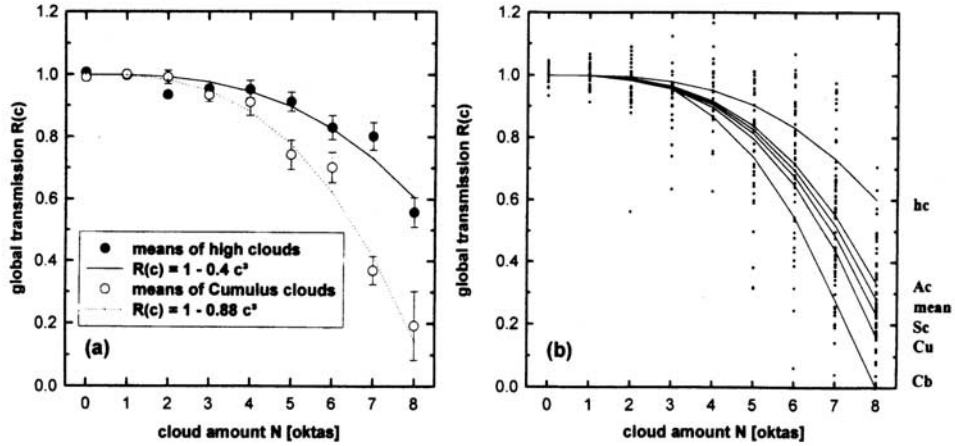

Figure 5. Cloud modification factors versus cloud cover. (a) Mean and standard deviation for each cloud amount and for high clouds and cumulus separately along with corresponding fitted curves. (b) All experimental values and fits for each cloud type category (hc, high clouds; Ac, altocumulus; Sc, stratocumulus; Cu, cumulus; and Cb, cumulonimbus) and for all cloud types together ("mean"). From *Thiel et al.* [1997], reproduced with permission of the American Society of Photobiology.

regression explained almost 56% of the variance. Moreover, when visibility was included as an additional independent variable, the explained variance of the corresponding regression was raised to almost 65%. In conclusion (according to *Frederick and Steele* [1995]), if no information about Sun screening is provided, simple models for cloud effect are limited to explaining around 65% of the variance.

[50] The work by *Josefsson and Landelius* [2000] introduces the use of concurrent human observations of clouds and measurement of sunshine duration and total solar radiation in order to analyze the relative effect of clouds on erythemal UV irradiance. When considering only cloud cover, they found again that cloud effect is very low for cloud amounts less than 4 oktas. For overcast conditions, mean CMF was 0.35. The typical large scatter of values was maximum at cloud amounts of 5–7 oktas. According to *Josefsson and Landelius* [2000], besides the earlier described factors (actual optical thickness and relative position between Sun and clouds), two other reasons can contribute to the scatter of values: different time basis for radiation measurements and cloud observations and cases with snow-covered ground surface. The study of cloud effects for different cloud types was approached by classifying clouds into four clusters: high clouds (H), all middle and low clouds (LM), LM without precipitation (LMnp), and LM with precipitation (LMp). Obviously, they found that high clouds almost do not affect UV radiation, while, at the other extreme, precipitating clouds may reduce more than 70% of UVE irradiance.

[51] Similarly, *Krzyscin et al.* [2003] found (see Figure 6) that almost no effect exists for high clouds, while the strongest effect is due to low clouds, with a mean CMF of 0.53 for overcast conditions. Among low-clouds cases, overcast skies with nimbostratus (sometimes combined with Sc) result in the greatest attenuation, with CMF values around 0.3 (0.1 during precipitation events). Middle clouds, with a CMF value of 0.63 for 7–8 oktas, can reduce UVE considerably more than high clouds. Similar results were previously reported by *Kuchinke and Nunez* [1999]: For cirrus clouds, mean CMF = 0.95, while for stratus and cumulus of bad weather, mean CMF = 0.16. Kuchinke and Nunez also studied the effect of SZA on cloud attenuation and suggested two different fits (see Table 4) for different ranges of SZA. Specifically, they found that cloud transmission of UV irradiance decreases with increasing SZA.

2.3. Methods Based on Nonhuman Observations of Clouds

[52] The longest databases of cloudiness observations are established from visual (human) observations. These data, however, have three problems: subjectivity, low frequency,

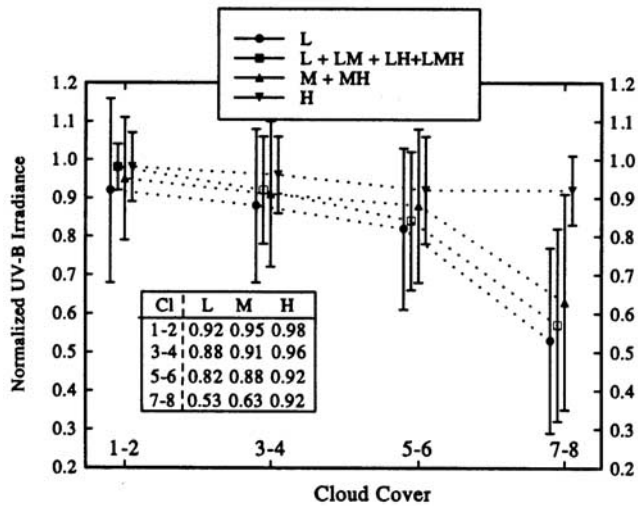

Figure 6. Mean CMF, i.e., normalized irradiance (±1 standard deviation) versus cloud cover for different cloud types (H, high clouds; M, middle clouds; and L, low clouds). From *Krzyscin et al.* [2003], reproduced with permission of Elsevier.

and no exact correspondence with any automatic measurement. Relatively modern alternatives to visual observations are ground-based sky cameras and satellite cloud retrieval techniques. However, both systems present some problems too. Ground-based sky cameras have systematic detection errors such as misdetection of thin clouds and limitations in distinguishing cloud type. Satellite cloud retrievals have a top-down vision, different from the bottom-up vision of human observers and radiometers. Moreover, they have either spatial (geostationary satellites, which are forced to orbit around the equator) or temporal (polar satellites) resolution restrictions and detection inaccuracies over high-albedo surfaces. Although satellites make possible a global coverage of cloud observations and the retrieval of cloud microphysical characteristics, which might be important for the improvement of cloud effect studies, we have limited the present review to ground-based techniques. Therefore in this section we shall present some studies about relationships between UV radiation measurements and cloud observations obtained by sky cameras.

[53] After some pioneering works [e.g., *Burkowski et al.*, 1977] we can first mention a more recent paper by *Schafer et al.* [1996], who established that cloud effects on UV radiation can sometimes be larger than ozone-induced changes and commented on difficulties associated with the highly irregular nature (spatial and temporal) of clouds. They suggested the use of a wide-lens video camera to keep continuous (i.e., high temporal resolution) track of cloud characteristics over a site, including cloud amount, type, and degree of Sun occultation. These characteristics were visually (i.e., subjectively) determined from the recorded images. In the further analysis, only stratiform and cumuliform clouds were included, since cirriform clouds were often not detected on the video images. Although information about cloud type was available, *Schafer et al.* [1996] studied only the dependence of CMF on cloud amount and SZA. Assuming that cloud effects are negligible for cloud amount less than 4 tenths, they used five clusters of cloud amounts: clear sky, 4–5 tenths, 6–7 tenths, 8–9 tenths, and overcast. CMF turned out to be independent of SZA for overcast conditions, while for other cloudy conditions CMF increased by approximately 17% when SZA increased from 30° to 60°. The mean CMF for all SZA is close to the average for data taken at 50°. Specifically, CMF at 50° is 0.788 ± 0.076 for 4–5 tenths of cloud cover, 0.747 ± 0.075 for 6–7 tenths, 0.614 ± 0.068 for 8–9 tenths, and 0.296 ± 0.025 for overcast conditions. Note the lower variability of values when approaching overcast conditions. Schafer et al. defined a third-degree polynomial that fits the empirical points obtained at SZA = 50° (see Table 4). Another contribution of this work was a detailed study of UVB cloud enhancement cases. *Schafer et al.* [1996] found that this phenomenon never occurred when the Sun was obscured by clouds (recall that cirriform clouds were not included in the study). Measured enhancements were as high as 11% and were related by the authors to reflections at cloud edges, which depend on Sun-cloud relative position.

[54] Another extensive work developed using ground-based sky cameras was carried out in Australia and was summarized by *Sabburg and Wong* [2000b]. In order to record the sky condition a wide-lens (116.5° field of view) sky camera was mounted on a Sun tracker, and it took sky images every 6 min. A piece of software that automatically extracted comprehensive information from each video image was developed. Several properties were retrieved, including solar disk obstruction, cloud cover, and cloud brokenness. Disk obstruction was used to select the cases when the Sun was occulted by clouds, which were the cases included in the further analyses. Relations between each sky property and CMF were investigated independently. This means that all properties except the one under scrutiny were set within a narrow range of values. For each case a best fit curve (second-degree polynomial) was obtained. Then, a sky formula (i.e., an expression that may be used to modify cloudless sky modeled irradiances to obtain estimations of real (cloud affected) irradiances) was proposed by combining all fitted expressions. The sky formula was applied to show that its use improves the modeling of UVB irradiances when compared to the cloudless sky model alone.

[55] Cloud information from pictures taken by a camera was used by *Grant and Heisler* [2000] to estimate UV radiation under any sky condition. Specifically, cloud fraction f and cloud type were derived from visual inspection of hemispherical photographs taken before and after each period of UV measurement. When f was compared to cloud cover directly observed at a weather station, they found that f was underestimated for high-cloud fractions and overestimated for low fractions. This result should be taken into account when f is used in the analyses. When plotting CMF versus f, no important cloud effect was found for $f < 0.7$, except at $f \sim 0.5$. This relative minimum was explained as the result of counteracting effects: increased probability of Sun obstruction and increased scattering from the side of clouds with increasing cloud cover. For overcast sky the mean CMF was as high as 0.65. *Grant and Heisler* [2000] suggested a linear fit, which was justified according to the following development. The temporal average of UVB irradiance in partly cloudy sky is a combination of contributions from a cloudless sky (UVB_{cl}) and an overcast sky (UVB_{ov}):

$$UVB = (1 - f)UVB_{cl} + fUVB_{ov}. \quad (8)$$

This approximation does not take into account reflections at cloud boundaries, reflections between clouds and ground, and Sun obscuration. Dividing equation (8) by UVB_{cl} and rearranging, we obtain

$$CMF = 1 - f\left[1 - \frac{UVB_{ov}}{UVB_{cl}}\right]. \quad (9)$$

Therefore, if the ratio of irradiance for overcast skies to cloudless skies is constant, the bracketed factor in equation (9) is constant and corresponds to the slope of the regression line between CMF and cloud fraction. With

their data, *Grant and Heisler* [2000] found that the best fit (with a very low $r^2 = 0.27$) corresponded to an intercept value of 1.08 (instead of the theoretical 1.00) and slope equal to −0.36. Note that these values correspond to a value of 0.64 for the ratio UVB_{ov}/UVB_{cl}.

2.4. Methods Based on Radiative Measurements Only

[56] It has been shown in sections 2.1–2.3 that cloud effect on UV radiation depends highly on both cloud amount and cloud type. However, great limitations exist on availability and suitability of cloud data both from human observations and from automatic devices. Therefore reconstruction of UV radiation time series using cloud observations involves large uncertainties. It would be very convenient to be able to estimate UV radiation from other data usually and historically measured, so an alternative approach has been studied by some researchers. This approach assumes that some relationship can be found between cloud effect on UV radiation and cloud effect on total radiation since the latter is also affected by clouds. Actually, some authors have established that CMF for total radiation is a good independent variable for estimating CMF for UV. For example, *Frederick and Steele* [1995] used a linear regression model and found that more than 90% of variance could be explained. Several studies that share this basic assumption are reviewed below. Unfortunately, it is difficult to compare results from these studies with results from works in sections 2.1, 2.2, and 2.3 since there is no unique correspondence between cloud cover and total solar radiation.

[57] A typical example of this kind of study is the paper by *Bordewijk et al.* [1995], who aimed to estimate biologically effective UV radiation in all-sky conditions with a simple approach based on an empirical relation between cloud effect on the UV band and cloud effect on total solar radiation. Therefore the CMF definition was applied both for UV doses and for total solar radiation (CMF_{tot}), the latter being considered a measure of cloudiness. A radiative transfer code, which considers actual daily ozone column and typical values for ground albedo and aerosol load and profile, was used to compute cloudless sky UV doses, and a simple parameterized function was used to estimate cloudless total irradiance from solar zenith angle. Comparison between CMF and CMF_{tot} for several instantaneous cases is shown in Figure 7. The authors highlighted the different behavior of the broadband and UV; when total solar radiation is largely attenuated (20–30%), UV dose may remain almost as in cloudless skies. High "reduction" factors (up to 1.3, i.e., enhancements) were found, and the authors established that these could be due to reflections in cloud boundaries or to the presence of thin cirrus. The analytic curve that fits the points is given in Table 4.

[58] Similarly, *Bodeker and McKenzie* [1996] investigated the relation between cloud effects on UV and total solar radiation as a response to the challenge of including cloud effects on estimates of UV radiation. Like other studies they used two ratios between measured irradiance and cloudless sky estimation of irradiance: one for erythemal UV (CMF) and the other for total solar radiation (CMF_{tot}). The division between these ratios was called cloud cover modifier (CCM). Therefore the CCM takes into account the specific cloud effect on UV. In order to estimate cloudless sky irradiances, two different methods were used: an empirical formula depending on solar zenith angle and a radiative transfer code including ozone column, water vapor, turbidity, surface pressure, temperature, and humidity. For both methods, however, results about cloud effects are similar. *Bodeker and McKenzie* [1996] focused on variability of cloud effect as a function of SZA. To do so, they plotted CMF versus CMF_{tot} for all data corresponding to a narrow range (1°) of SZA. One such plot is reproduced in Figure 8. Observing the scatter of points in these plots, and based also on theoretical arguments, four cases were distinguished in the analyses: (1) cloudless sky (points with CMF = CMF_{tot} = 1.0); (2) overcast sky (CMF = CMF_{tot} < 1.0); (3) partly cloudy with the Sun obscured (CMF_{tot} < 1.0 and CMF > CMF_{tot}); and (4) partly cloudy with the Sun not obscured (CMF_{tot} > 1.0 and CMF < CMF_{tot}). Results of this work are analytical expressions that fit the data (see Table 4) in such a way that cases with CMF_{tot} greater or less than 1.0 are treated separately. The values for the coefficients in the expressions, which depend on SZA, are presented through several figures by *Bodeker and McKenzie* [1996]. A similar expression, but for all SZA, was suggested by *Matthijsen et al.* [2000] in a paper devoted to comparing satellite and ground-based approaches to estimate UV radiation (see Table 4). Another expression to relate CMF with CMF_{tot}, which is in this case a second-order polynomial (see also Table 4), was suggested by *Krzyscin et al.* [2003] in a paper already reviewed (see section 2.2). As in earlier studies these authors found higher cloud effect on total irradiance than in UV.

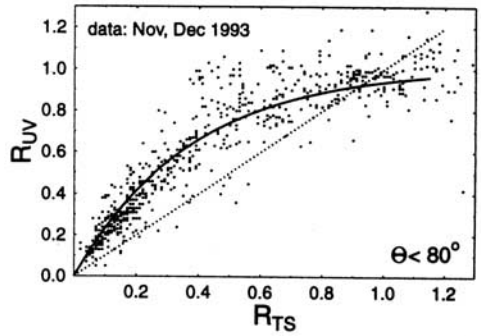

Figure 7. Reduction factor (i.e., CMF) for UV doses versus the same ratio for total solar irradiance. From *Bordewijk et al.* [1995].

[59] Going deeper with the relationship between broadband and UV measurements, *Foyo-Moreno et al.* [1999] investigated, first, the fraction of UV radiation within the total solar radiation. They found mean values from 3.7 to 4% for this fraction. More interestingly, most cases with high UV fraction corresponded to low broadband irradiances and low clearness index values. The clearness index k_t is defined as the division between measured broadband irra-

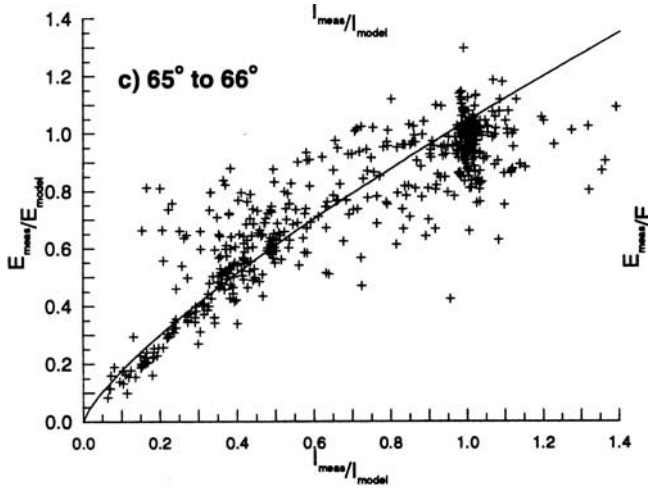

Figure 8. Cloud modification factor for UV versus the same for total solar irradiance for values taken at SZA = 65°–66°. Curve obtained with the corresponding fit (see Table 4), extrapolated to values of $CMF_{tot} > 1.0$, is also shown. From *Bodeker and McKenzie* [1996], reproduced with permission of the American Meteorological Society.

diance and extraterrestrial irradiance and is used as a surrogate for cloud optical thickness. Since k_t is a value of transmittance that takes into account the effect of clouds, the latter result confirms the higher cloud transmission within the UV band. Second, *Foyo-Moreno et al.* [1999] suggested several methods to estimate UV radiation from typical measurements. The best one (according to the authors) is quite simple: In a first step, cloudless UV irradiance is estimated by a simple formula; in a second step the cloudless irradiance is modified by an expression that accounts for both broadband transmissivity of the atmosphere (parameterized through k_t) and specific effects in the UV band (see Table 4).

[60] The work by *Nann and Riordan* [1991] reveals two important differences from the papers reviewed above: First, it focuses on spectral dependence of cloud effects, and, second, it aims to establish a model for irradiances (including UV, VIS, and IR bands) on south tilted surfaces. For these analyses they used a spectrally dependent transmission ratio $R(\lambda)$ defined as the ratio of measured monochromatic irradiance to a standard reference irradiance. Nann and Riordan found that in overcast conditions, ratios for the shortest wavelengths are significantly higher than for the rest of the spectrum. Actually, in the UV and VIS regions, $R(\lambda)$ decreases almost monotonically as wavelength increases. The model developed by *Nann and Riordan* [1991] was based on an already available radiative transfer code [*Bird and Riordan*, 1986] that allows calculating the cloudless sky spectral irradiance. The effect of clouds was introduced in two steps: (1) The whole spectrum was modified by the broadband cloud effect. (2) A cloud cover modifier (CCM) was applied to introduce the spectral dependence of cloud effect. Note that CMF, as defined in this review, would be the product of the broadband cloud effect by the CCM, integrated over the UV band. CCM was calculated using a second-degree polynomial fit that was obtained over the available spectra and that allows calculating the CCM for each wavelength as function of the clearness index k_t.

2.5. Methods Based on Both Radiative Measurements and Observations of Clouds

[61] Some studies combine cloud observations with radiation measurements both in the UV and in the solar broadband to derive the CMF. For example, *Blumthaler et al.* [1994b] plotted the ratio between CMF for UV radiation and CMF_{tot}, as function of cloud cover. They found that CMF for erythemal UV may be 1.5 times the corresponding CMF_{tot}, when solar elevation is low and sky is overcast. The ratio between both factors is 1.3 when averaged for all Sun elevations and for overcast conditions. Maximum ratios of almost 2.0 were found in broken cloudy conditions when the Sun is obscured by clouds.

[62] With the aim of investigating the effect of clouds and haze on UVB for improving the UVI forecast in the United States, *Estupiñán et al.* [1996] combined measurements of UV radiation with measurements of broadband solar radiation and observations of cloud cover and cloud type that were available at a nearby weather station. They worked on a so-called UV attenuation α_B, that can be easily related to CMF (CMF = 1 + α_B). Usually, α_B is negative (a positive value means enhancement). Regarding the broadband irradiance, they tried both the CMF_{tot} and what they called the total solar transmissivity T_s (the clearness index for other authors). High correlation ($r = -0.93$) between α_B and T_S and also between α_B and cloud cover C ($r = 0.60$) was found. Therefore *Estupiñán et al.* [1996] adjusted an analytical expression (see Table 4) that relates the three magnitudes. An interesting characteristic of this expression is that it can produce cloud enhancements of UV radiation when $T_s > 0.7$ and $C > 5$ tenths. Indeed, a detailed report of enhancement cases that produced UVE values 20% higher than the cloudless sky estimation showed that most of them occurred with cloud cover between 6 and 9 tenths and transmissivity between 0.7 and 0.9. Cumuliform clouds (cumulus or cumulonimbus), with or without middle and high clouds, were observed in all these cases. Similarly, *Trepte and Winkler* [2004] derived CMF with the goal of reconstructing a long-term series of UVE irradiance. They used sunshine duration data to separate cases of visible Sun and obscured Sun. For the latter cases they established second-degree polynomial fits depending on SZA (see Table 4) to parameterize the dependence of CMF on CMF_{tot}. In this work, CMF included the effect of aerosols, since the clear-sky reference for both UV and total radiation were estimated for a cloudless, aerosol-free atmosphere.

[63] We have already commented on a paper by *Grant and Heisler* [2000]. Some of the methods that they proposed were based on the use of a photosynthetically active radiation (PAR) sensor, which measured the photon flux density with maximum sensitivity at 660 nm. They

checked several methods relating UVB and PAR measurements: For example, they found $r^2 = 0.68$ for a linear regression between CMF and CMF_{PAR}. In order to improve this result they checked a formulation based on observations of clouds from sky images (see section 2.3). In this method, equation (9) was modified in the sense that cloud fraction f was substituted for the probability of a cloud obstructing the Sun (P_{cld}). This probability is related to sunshine duration but was estimated from the PAR measurements. Linear regression of CMF with P_{cld} resulted in a low correlation $r^2 = 0.21$, which only improved to 0.32 when the highly scattered values for overcast conditions were excluded. The last approach by *Grant and Heisler* [2000] was the most physically realistic; in this approach, direct beam and diffuse components were treated separately. After a theoretical development (not reproduced here) and introducing some corrections to account for residuals caused by otherwise unaccounted for 3-D scattering phenomena (e.g., cloud edges), they obtained the following expression:

$$\mathrm{CMF} = 1 + P_{cld}\left(\hat{D}_{cl} - 0.86\right) + f\left(0.09 - \hat{D}_{cl}\right) + f \sin \mathrm{SZA}, \quad (10)$$

where $\hat{D}_{cl}$ means diffuse fraction (i.e., the ratio of diffuse UVB irradiance to global UVB irradiance) computed for cloudless conditions. Grant and Heisler used the appropriate records from their database to calculate the coefficients that appear in the formula. The diffuse component $\hat{D}_{cl}$ is to be computed by using a radiation model (they suggested the one by *Schippnick and Green* [1982]). This expression accounted for 60% of the variability in the data ($r^2 = 0.6$) when applied to the UVB data with solar zenith angles between 18° and 71°.

[64] The paper by *Schwander et al.* [2002] explored the use of the neural network methodology to estimate CMF from several parameters related to clouds and atmospheric state. The main advantage of neural networks is the ability to reproduce nonlinear relations between input and output after a training process, without a priori functional dependency needed. Assuming that CMF is slightly spectrally dependent within the UV band, Schwander et al. studied six particular wavelengths in the UVA and UVB (from 300 to 380 nm). When a single CMF value was given, it meant the average of the six monochromatic values. Five different neural network configurations were trained for five different sets of inputs. These inputs included cloud information and total solar radiation measurements, along with other data such as albedo and SZA. The quality of these neural network estimates was evaluated through their mean absolute error (MAE) and by means of plots of predicted CMF versus observed CMF (see Figure 9). When both cloud information and total solar radiation data were used, results turned out to be much better than when only cloud amount was used (MAE = 0.073 and MAE = 0.141, respectively). In addition, the former neural network can predict enhancements and attenuations below 0.25. Unfortunately, given the nature of neural networks, these results cannot be reduced to a simple analytical expression. Regarding the spectral dependence of CMF values, *Schwander et al.* [2002] found that for overcast conditions and low clouds, CMF values increase with decreasing wavelength, and below a maximum at around 310 nm they decrease again. According to Schwander et al., two counteracting effects (increasing optical depth of air molecules with decreasing wavelength and enhanced tropospheric ozone absorption in the presence of clouds for wavelengths less than 310 nm) explain this behavior.

3. SUMMARY

[65] Almost all studies reviewed here use the same quantity to evaluate the cloud effect, although there is no agreement about its name. This quantity is defined as the ratio of measured radiation in cloudy sky to that calculated radiation for cloudless sky. Among all suggested names we have chosen cloud modification factor (from *Schwander et al.* [2002], also used, for example, by *Trepte and Winkler* [2004]), which is better suited to the actual behavior of the cloud-radiation interaction than other names such as cloud attenuation factor or UV reduction function that seem to imply an attenuation effect only. Other suggestions such as normalized radiation or irradiance ratio have no explicit reference to clouds. Finally, some authors use cloud cover modifier, which can be confusing since cloud cover is a measure of the amount of clouds occupying the sky hemisphere, while cloud effects on radiation may depend also on other cloud features. We must note that high CMF values (close to 1) correspond to low cloud effect, while low CMF values correspond to high cloud effect.

[66] The contents of Table 4 (i.e., characteristics and results of the studies reviewed in this paper) will be the basis for most of the comments that follow in this summary section. In addition, comparison of cloud effects according to the reviewed works is presented in Figure 10 (for those CMF that are given as a function of cloud cover) and Figure 11 (for those CMF that are given as a function of the cloud effect on total solar radiation). Figures 10 and 11 will also be discussed below.

[67] One of the differences (not included in Table 4) among the reviewed works is their specific motivation. We have been able to classify motivations into the following groups: (1) development or reconstruction of UV climatic databases (either from cloudiness or from broadband radiative measurements), (2) studies about cloud-UV interaction at climatic timescales (e.g., comparison of cloud and ozone induced variability), (3) studies about cloud-UV interaction at short timescales (usually health related), and (4) UV index forecasting for any sky conditions.

[68] Any of these objectives drives the development of a parameterized mathematical model that relates the specific UV variable (UVE, UVB, UVI, etc.) in cloudy skies with some input parameters related to clouds. These relationships

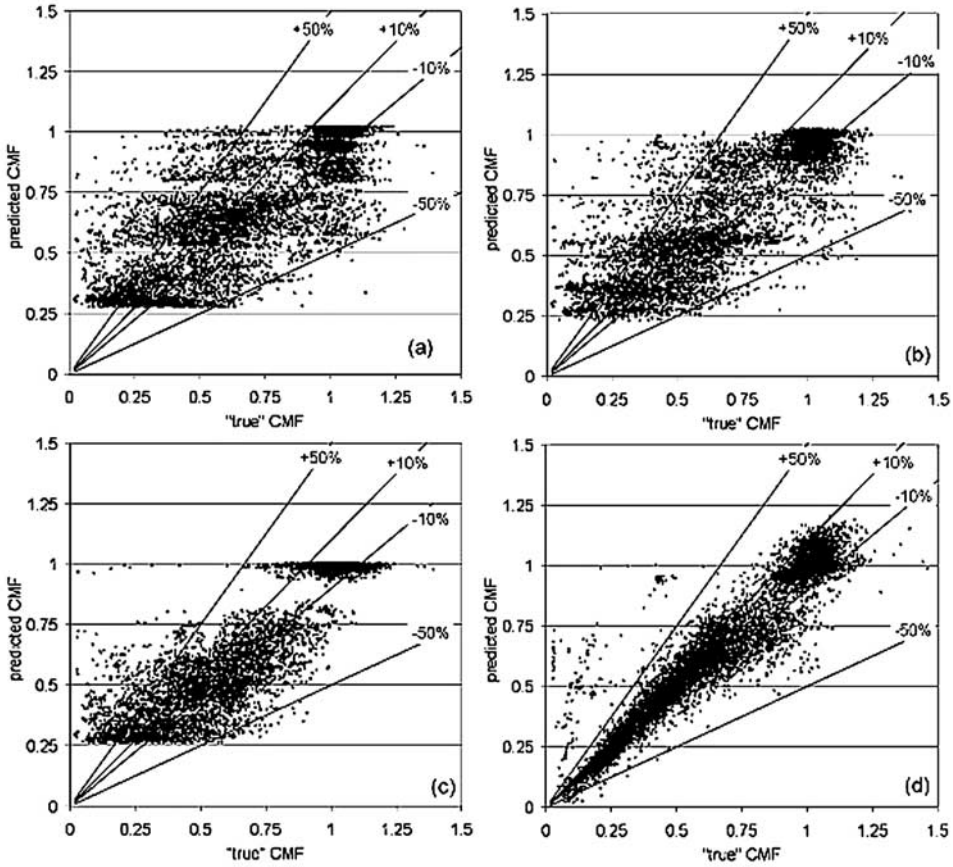

Figure 9. Scatterplot of predicted CMF versus observed CMF by the neural networks that use (a) SZA, ground albedo, and total cloud amount. (b) Same as Figure 9a plus cloud amount and type for three layers. (c) Same as Figure 9b plus a flag whether solar disk is obscured or not. (d) Same as Figure 9a plus visible irradiance. From *Schwander et al.* [2002].

(cloudy models) must be derived from a database that includes simultaneous measurements or observations of the UV quantity and the input parameters. Therefore the length of the database should be long enough to assure statistical meaning. In the reviewed works the length of the database is from only 60 records [*Josefsson*, 1986] up to 35,000 samples [*Josefsson and Landelius*, 2000].

[69] Regarding the spatial coverage of the data used, most works base their analyses and results upon one measurement site only. Notable exceptions to this fact are the works for the United States [*Long et al.*, 1996] and Sweden [*Josefsson*, 1986]. Very few works [*Burrows*, 1997; *Schwander et al.*, 2002] distinguish between a database for developing the CMF parameterization and another database for testing it. Therefore the portability of cloudy models is, in general, not investigated. Last, but not least, most works are for northern midlatitudes in Europe and North America, while there are only four works for the Southern Hemisphere (including two in Australia, one in New Zealand, and one in Antarctica). The only work that uses data in the tropics (Malaysia) is the one by *Ilyas* [1987].

[70] Most of the reviewed works apply some limitation in the data used, based on the solar zenith angle. Generally, this limitation is set to 70° or 80° and justified because of low accuracy of the cloudless model and/or poor cosine response of the instrument used for measurements. Other works analyze data in a narrow range of SZA. Finally, some other papers address the effect of the SZA on the cloud effect, i.e., suggest different values or fits depending on the SZA. This factor (the treatment of the SZA) is to be taken into account when comparing results of the above reviewed papers and when using them.

[71] The time basis of measurements (or their averages) should be chosen according to the aim of the work, so for climatic purposes monthly or yearly bases might be adequate, while daily or shorter time bases should be used for UVI forecasting. Time bases in the reviewed works vary from instantaneous (meaning the time required to perform the measurement or the spectral scan) to 1 day. The only exception is *Ilyas* [1987], who uses 1 month as the time basis. Most authors use averaging times between 5 min and 1 hour. However, cloudiness observations are usually instantaneous, so authors are actually relating the averaged UV irradiance in a period of time with an instantaneous cloudiness observation performed more or less in the middle of the time interval. If sky conditions change considerably during the averaging time, the match-

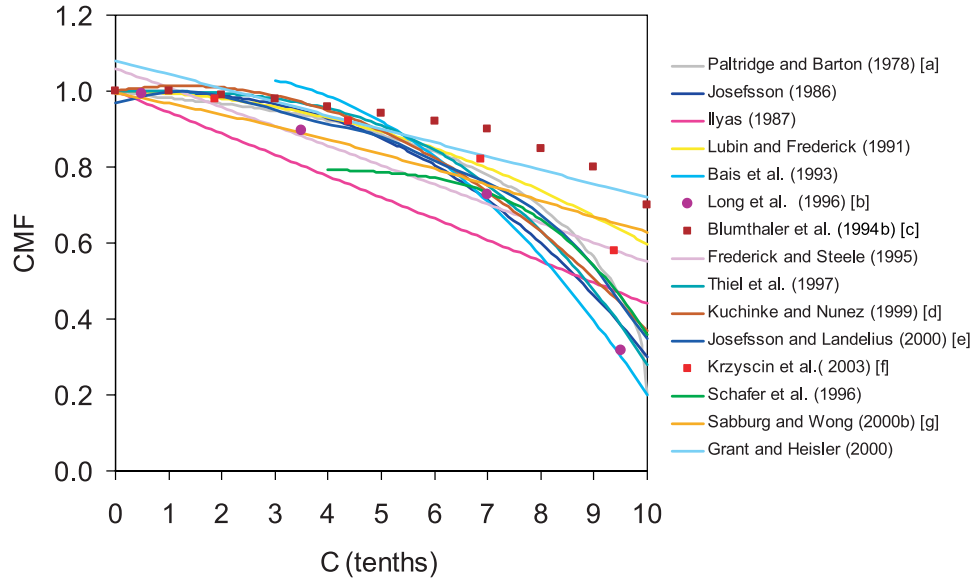

Figure 10. Cloud modification factors for UV radiation versus cloud cover, as given by several reviewed papers. Note that different magnitudes (UVE, UVI, UVB, single wavelength, etc.) have been used when defining CMF in each work so lines plotted here are not strictly comparable. Except when noted, values are from the fitted formulae shown in Table 4. Legend notes indicate the following: a, from the curve drawn in the original paper; b, from CMF values given in the original paper for four sky conditions; c, from the plot for erythemal radiation in the original paper, values corresponding to all cases, i.e., not distinguishing cloud level; d, from the fitted formula for SZA in the range 35°–59°; e, from the plot in the original paper; f, from the plot in the original paper, values corresponding to all cases, i.e., not distinguishing cloud level; and g, from the sky formula set in the original paper. (For variables apart from cloud amount we have assumed the following values: Aureole brightness is 0.32, angle of maximum cloud cover is 37.5°, cloud brokenness is 0.25, and cloud brightness variation is 0.092.)

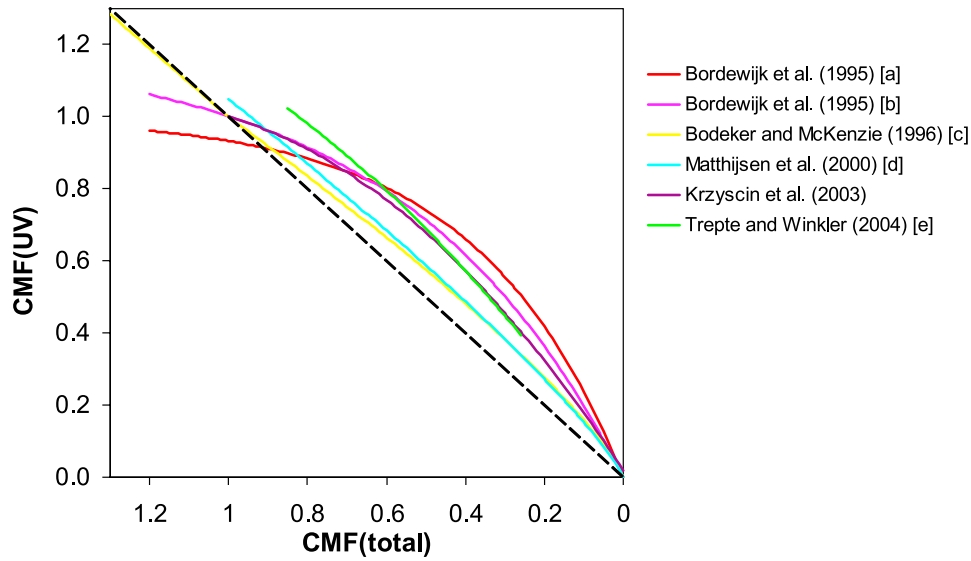

Figure 11. Cloud modification factors for UV radiation against the equivalent for total solar radiation, as given by several reviewed papers. Note that the values in the abscissa have been plotted in the reverse sense in order to allow a qualitative comparison with Figure 10. All works but one (*Bordewijk et al.* [1995] uses an action spectrum for carcinogenesis in albino mice) use erythemal UV when defining CMF. Dashed line corresponds to CMF = CMF_{tot}; it is shown here as a reference. The formulae used here to draw the curves are given in Table 4. Legend notes indicate the following: a, using coefficients for instantaneous measurements; b, using coefficients for daily averages; c, using $A = 1.0$ and $P = 0.8$, corresponding approximately to SZA = 60°; d, using coefficients given by the authors for their best fit; and e, using coefficients given by the authors for SZA = 50°.

ing of averaged radiation measurements with instantaneous cloud observations may turn into confusing results. Therefore low variability of cloudiness should be guaranteed when making use of an instantaneous measurement instead of an averaged value [*Schwander et al.*, 2002]. In this sense, short time bases are better suited to instantaneous sky observations. Of course, the problem disappears when using broadband irradiance measurements as the only input parameter, because both variables (UV and broadband irradiances) can be obtained with the same time interval.

[72] Still regarding time basis, we should note that a parameterization developed with some specific time basis data should not be used with values taken at a different time basis. The reason is that variability of both clouds and UV radiation is different at different timescales. If a given parameterization is used with data taken at a different time basis, an analysis of the induced error should be considered. Differences among cloud effects reported by the works reviewed here, however, are more related to uncertainties in measurements and models, different cloud types, etc. than to the time basis used.

[73] Regarding the dependent variable of the cloudy model, there is a large choice of options. Several authors use integrated UVB irradiance, either unweighted or weighted with the erythemal action spectrum (i.e., UVE). Other authors include the UVA band or analyze some single wavelengths. Finally, sometimes UV doses are also considered. The choice of the variable is related to the goal of the work but also to the available instrument. The most frequently used instruments are Robertson-Berger type radiometers, the Eppley UV sensor, and spectroradiometers. Cloud amount and total irradiance are the most frequently used independent variables (or input parameters). Cloud amount is generally reported from human observations, although it is widely recognized that human observations are highly subjective. Some works make use of sky cameras, which have some detection problems too. It is obvious that many uncertainties in CMF come from difficulties in detecting and/or estimating cloud physical or optical characteristics. Again, methods based on total irradiance avoid this problem, since measurements of total solar radiation are easily performed by standard pyranometers.

[74] One important input for establishing the cloud effect is what we call the cloudless model, i.e., the estimate of UV radiation in cloudless skies. First of all, note the difference between cloudless sky and clear sky. Cloudless is a word that defines precisely a sky without any cloud, while clear is an ambiguous word that can also be related to a low aerosol burden or even to good visibility. Provided that the goal of reviewed works is to establish the cloud effect on UV radiation, cloudless models should include all other important variables affecting UV radiation in the absence of clouds. We have already seen in section 1.5 that these variables are SZA, TOZ, aerosol optical depth, surface albedo, and others. In the reviewed papers most of these variables are considered, although the degree of depth in the analyses varies from just mentioning them to detailed work.

[75] The use of radiative transfer models (RTM) for estimating cloudless radiation is probably the most common approach among the reviewed papers [e.g., *Lubin and Frederick*, 1991; *Thiel et al.*, 1997; *Krzyscin et al.*, 2003; *Nann and Riordan*, 1991; *Bordewijk et al.*, 1995; *Bodeker and McKenzie*, 1996; *Schwander et al.*, 2002]. Probably the most important issue to have in mind when using RTM is the uncertainty that they can add to the computation of CMF. Indeed, according to *Weihs and Webb* [1997], typical uncertainties in input parameters may result in errors in cloudless UV radiation of around ±20% at 305 nm and around ±10% at 380 nm. This and other works [see, e.g., *Schwander et al.*, 1997] agree in establishing that the most sensitive input variable in a RTM for UV radiation is TOZ. Nevertheless, since TOZ is usually available with high accuracy, it turns out that the critical inputs are aerosol optical depth and (if snow is present) ground albedo. Regarding the use of RTM for UV radiation, it is worth mentioning here the works by *Van Weele et al.* [2000], where a benchmark to test the validity of models was established, and by *Koepke et al.* [1998], where several models were compared.

[76] Two other approaches for estimating cloudless radiation are based on the use of measured irradiances in cloudless skies at the same site(s) and by the same instrument used for obtaining cloudy measurements. One option is to compute averages among cloudless measurements corresponding to similar conditions of SZA and, sometimes, of TOZ [*Bais et al.*, 1993; *Blumthaler et al.*, 1994b]. The second option is the use of analytical functions fitted to cloudless measurements [*Paltridge and Barton*, 1978; *Josefsson*, 1986; *Josefsson and Landelius*, 2000; *Bodeker and McKenzie*, 1996; *Estupiñán et al.*, 1996]. This approach may be understood as the use of a strongly parameterized radiative model, with the advantage of being adjusted to available measurements. *Koepke et al.* [1998] called these methods empirical models for cloudless skies and found that they give good results but only for the atmospheric conditions for which they have been developed. One advantage of these two approaches is that they avoid possible bias in the cloud effect as a result of poor calibration of radiation instruments. Indeed, since both the cloudy value and the cloudless estimate are based on measurements taken by the same instrument, a more reliable relative effect is computed.

[77] Although it is difficult to say which is the best method to be applied in future studies, some comparison between the cloudless estimates and actual cloudless measurements (made with the same instrument that is used for cloudy measurements) should always be performed. This comparison should provide a measure of dispersion and bias parameters, both necessary to judge the ability of the cloudless model and the improvements associated with the cloud effect parameterization. In order to perform the comparison for the cloudless cases it is necessary first to identify the cloudless samples in the database. This is approached through visual inspection by many authors, but there are several objective methodologies in the litera-

ture [e.g., *Feister and Gericke*, 1998; *Long and Ackerman*, 2000] usually based on total solar radiation measurements (both global and diffuse components).

[78] As far as results of the reviewed works are concerned, we shall start here commenting on those works that established some relation between cloud effect and cloud cover. Most of these works show their results through plots of CMF versus cloud cover, and many of them also suggest an empirical fit to the points shown in the plot. We have included in Figure 10 all suitable cases, i.e., when values can be extracted from the original plots or when an empirical fit was provided by the authors.

[79] The most relevant characteristic of Figure 10 is dispersion of curves and points from different authors, particularly at higher cloud cover. These differences are partially related to a characteristic that is common in most original plots: the large dispersion (or variability) of particular CMF values corresponding to the same cloud cover. Several reasons can be claimed to be responsible for the observed differences (both among particular cases in one specific study and among different studies). The main ones follow:

[80] 1. Different UV quantities are used, i.e., different spectral ranges, action spectra, etc.

[81] 2. There are different climates: different cloud optical characteristics for the same cloud type or different frequencies for cloud types. For example, *Krzyscin et al.* [2003] affirmed that differences among reported CMF may be due to specific regional characteristics of cloudiness, so it is necessary to include some explanation about cloud climatology at each considered site.

[82] 3. Several (or all) cloud types are treated together.

[83] 4. Samples with occulted and visible Sun are treated together.

[84] 5. There are different time bases for radiative measurements.

[85] 6. Surface albedo effects cause discrepancies, in particular at sites where the ground is sometimes snow covered.

[86] 7. Different cloudless models are used.

[87] 8. Different restrictions are set in the data regarding SZA.

[88] 9. There are errors both in UV measurements and in cloudless model estimations. According to *Sabburg and Wong* [2000b] a typical uncertainty in CMF of ±20% can be expected because of these two factors.

[89] In general, for climate studies when bulk values of cloud effects are sought, a description of CMF depending exclusively on cloud cover might be good enough [*Paltridge and Barton*, 1978; *Josefsson*, 1986]. When short time bases are used, however, cloud type, cloud optical characteristics, and especially Sun screening are important sources of uncertainty in determining suitable CMF values. Several authors [e.g., *Bais et al.*, 1993; *Schafer et al.*, 1996] use cloud cover as the only parameter in their fits, but usually the same authors highlight the large dispersion among particular samples in their databases and cite some of the reasons listed above to explain it. Other authors, of course, analyze in detail the effect of relative position between clouds and Sun (i.e., Sun screening) and the differences in cloud effect related to different cloud types. More specifically, some works split their databases depending on cloud level (low, middle, or high) distinguishing sometimes between precipitating and non-precipitating clouds [*Blumthaler et al.*, 1994b; *Thiel et al.*, 1997; *Josefsson and Landelius*, 2000; *Krzyscin et al.*, 2003]. Regarding Sun screening, its effect seems highly related to time basis in such a way that the shorter the time basis the more important it is to distinguish between samples with and without occulted Sun [*Blumthaler et al.*, 1994b; *Sabburg and Wong*, 2000b; *Schwander et al.*, 2002].

[90] The two limits of possible cloud cover (cloudless and overcast) are particularly interesting to investigate when comparing results from different studies. As far as cloudless skies are concerned, the theoretical value is CMF = 1.0. There are, however, some works that, as a consequence of the mathematical fitting procedure, give slightly higher values (e.g., *Grant and Heisler* [2000], with CMF = 1.08) or lower values (e.g., *Josefsson and Landelius* [2000], with CMF = 0.97). Actually, it is apparent that the above mentioned large dispersion of results is less important for low cloud cover (less than 3 oktas or 4 tenths of sky). In the latter conditions most authors agree that, on average, cloud effect is very low, producing CMF values close to 1.0 (e.g., *Josefsson* [1986] found CMF = 0.84 in days that he classified as broken clouds).

[91] Regarding the CMF values suggested for overcast conditions, we can see (both in Table 4 and in Figure 10) that a large range of values is given by different authors. Indeed, values as low as CMF = 0.2 [*Paltridge and Barton*, 1978; *Bais et al.*, 1993] and as high as CMF = 0.7 [*Blumthaler et al.*, 1994b; *Grant and Heisler*, 2000] are found. In general, the highest values are associated with sites where thinner clouds are to be expected: a high mountain site [*Blumthaler et al.*, 1994b] and a site in Antarctica [*Lubin and Frederick*, 1991]. The most common values found for CMF in overcast conditions are around 0.3. All works that distinguish different cloud types agree that cloud effect is reduced (CMF higher) when clouds are higher in the atmosphere. So usually CMF for high clouds is around twice the value for low clouds. For example, *Frederick and Steele* [1995] found CMF = 0.81 for overcast with high clouds, while for the lowest clouds, they found CMF = 0.40. *Thiel et al.* [1997] found CMF = 0.6 for overcast with high clouds, while for cumulonimbus clouds CMF was virtually 0. *Josefsson and Landelius* [2000] showed CMF = 0.7 for high clouds and CMF = 0.3 for low and middle clouds with precipitation. These results are in agreement with studies based on radiative transfer models, which obviously anticipate larger cloud effect for the larger cloud optical depth usually found for low clouds.

[92] Most of the mathematical expressions suggested for CMF reflect the behavior of cloud effect as a function of cloud cover by using a polynomial expression. In particular,

the most common empirical expressions are either second-degree polynomials [*Bais et al.*, 1993; *Kuchinke and Nunez*, 1999] or expressions based on the one suggested by *Kasten and Czeplak* [1980] for cloud effect on total solar radiation, with the power parameter in the range of 2.5– 3.5. Moreover, some CMF versus cloud cover relationships are virtually equal [*Josefsson*, 1986; *Thiel et al.*, 1997] even though they have been found with different time basis data. There are some authors, however, who suggest simple linear fits to the data [*Ilyas*, 1987; *Frederick and Steele*, 1995; *Grant and Heisler*, 2000], although these fits usually produce a too low cloud effect for broken or overcast conditions and a too large cloud effect for low cloud cover. Some authors provide a measure of the agreement between the fit and the original points. Typically, the coefficient of determination r^2 is the selected measure. Values of $r^2 \sim 0.7$ are sometimes found [e.g., *Thiel et al.*, 1997], although lower correlations are more common. However, this coefficient, and any other that is suggested and computed by the authors, cannot be used to compare the ability of different expressions, since they are always computed from the same database that was used to generate the empirical function. A proper comparison among different CMF values should be addressed in future research by using independent databases.

[93] Some of the above comments apply also to results of works that relate cloud effect on UV radiation with cloud effect on total solar radiation (including cloud observations or not in the analyses). Regarding these techniques, Figure 11 shows plots of all suitable cases, i.e., when an empirical fit is provided by the authors. In Figure 11 the scale in the abscissa axis has been plotted in reverse sense in order to obtain curves similar to the ones obtained in Figure 10. Indeed, high cloud cover values in Figure 10 correspond in general to low CMF_{tot} in Figure 11. Curves in Figure 11 show some variation, partly reproducing the dispersion that has already been found in the previous works based on cloud cover observations. However, all of them follow quite similar behavior. The most important feature of the relation between cloud effect on UV radiation and on total solar radiation is that the former is in general lower than the latter. This fact is made apparent in Figure 11 by comparing suggested curves with the reference line that would correspond to identical cloud effects: In general, given a particular sky condition, CMF is higher that the corresponding CMF_{tot}. According to the reviewed works this is particularly true when cloud cover is large and the cloud optical depth is also large (i.e., when $CMF_{tot} < 0.4$). In these cases, CMF for UV radiation might be almost twice the value for total radiation. Another common conclusion from all works that use total radiation for establishing a cloudy model for UV radiation is that results of applying such a model are much better than results of models based on cloud cover observations only. This is due to the fact that total radiation measurements are indirect observations of cloud optical depth and Sun screening, which are not available when only cloud cover is used.

[94] Another issue is the wavelength dependence of cloud effect within the UV band. In general, earlier studies agreed that CMF had no significant wavelength dependence, but more recent analysis has shown some evidence contrary to that statement. For example, *Seckmeyer et al.* [1996] developed a study of the transmissivity through a stratified cloud, with measurements above the top and below the bottom of the cloud. They found transmittance of 60% in UVB and 45% in UVA, i.e., CMF lower in UVA. The same team reproduced these results using a radiative transfer model and proposed the conclusion that the origin of the differences lies in photons that are backscattered to the atmosphere at the top of the cloud and then suffer Rayleigh scattering. This scattering is larger at shorter wavelengths, so there is more scattered light at shorter wavelengths that returns from the atmosphere to the cloud. Then, this light suffers an almost grey (i.e., uniform wavelength) transmission through the cloud. So the final result is a relative increase of radiation at shorter wavelengths [*Kylling et al.*, 1997]. Moreover, *Mayer et al.* [1998] showed that in the presence of thick clouds, coupling of cloud scattering and molecular or particulate absorption can result in a strong enhancement of absorption, which may appear as a wavelength dependence of cloud attenuation. Among the works reviewed in the present paper, only a few of them searched for wavelength differences. We can mention *Nann and Riordan* [1991] and *Blumthaler et al.* [1994b], who confirmed higher CMF at shorter wavelengths, and *Schwander et al.* [2002], who found maximum CMF at 310 nm, compared to CMF at other wavelengths in the range 300–380 nm. The latter result is important in the sense that wavelengths around 310 nm are the strongest contributors to the erythemal irradiance.

[95] A particular comment is required regarding the cloud enhancement effect. This effect is the increased solar radiation levels (both in the UV and in the broadband) that are sometimes found under partly cloudy and even overcast conditions. Enhancements are explained basically by two phenomena: reflections in cloud surfaces and increased forward scattering in some types of clouds. Enhancement depends in some way on measurement time basis, although almost all reviewed works have some data that reflect such enhancement effect in the UV band (see Table 4). Actually, measurements from the reviewed papers show some enhancements as high as 20% and even, exceptionally, 30% above the expected cloudless radiation [*Bordewijk et al.*, 1995]. The enhancement effect merits different attention depending on each author: In some cases no comments are made, while in other studies a quite deep analysis is included. Actually, some works try to establish the CMF not only in the usual range of reduction effect but also for the enhancement cases [*Burrows*, 1997; *Bordewijk et al.*, 1995; *Estupiñán et al.*, 1996; *Schwander et al.*, 2002]. The UV cloud enhancement effect has received a lot of attention among the scientific community in recent years, so a long list of papers that deal with it can be provided. The present review, however, has not covered papers that focus attention on the enhancement effect since that was beyond our scope. For the interested reader a broad review of cloud

enhancement effects in the UV band is given by *Parisi et al.* [2004].

4. CONCLUDING REMARKS AND GENERAL RECOMMENDATIONS FOR FUTURE STUDIES

[96] In this paper we have reviewed a number of studies that suggest some quantification for the ratio between a UV magnitude in cloudy skies and the same magnitude in cloudless conditions. To our knowledge, most papers published at the time of writing this review have been included. Some works that focus on a particular component of radiation have not been included (e.g., *Grant and Gao* [2003] put their attention on the diffuse fraction of UV radiation). Works focused on satellite-based approaches [e.g., *Williams et al.*, 2004] have not been included either. The reviewed relationships have been compared, through the use of a common variable, the so-called cloud modification factor (CMF). The range of CMF values found within the reviewed papers is very large, especially at broken and overcast conditions and owing to the broad range of sites, climates, temporal basis, UV variable concerned, instrumentation, etc. Most authors agree that difficulties in describing cloud effects on UV radiation come basically from the large variability of cloud fields (sky condition) either in space, time, cloud type, or optical characteristics. Nevertheless, some common facts can be stated and are given here.

[97] 1. Cloud effect on UV radiation is lower than cloud effect on total solar radiation. In other words, given a sky condition, the CMF is in general higher for UV radiation than for total solar radiation.

[98] 2. There is a large dispersion of CMF values corresponding to the same cloud cover even for a single site and period of time. This is not surprising since cloud cover is a quite poor description of sky condition: Different cloud types, different cloud optical depths, different relative position of the Sun with respect to clouds are possible within the same observed cloud cover.

[99] 3. If short timescales are involved and an accurate description of UV radiation for cloudy sky is required, total (broadband) solar radiation is the best input parameter.

[100] 4. The cloud effect on UV radiation is usually a reducing effect. There are, however, a significant number of cases when the effect of clouds is to increase the UV radiation at the surface. This phenomenon, called enhancement effect, has been investigated recently in detail.

[101] 5. Two main shortcomings appear in the reviewed works. First, there is limited spatial coverage in the databases used (most works are built on data from northern midlatitudes; a few are built on other sites of the world). Second, most works that suggest an empirical formula to estimate CMF do not check the validity of the formula on an independent data set (i.e., validation tasks and portability tests are missing in most works).

[102] Finally, we suggest some recommendations here that might be considered for future studies addressing empirical analysis of interaction between clouds and UV radiation.

[103] 1. Clearly establish and accurately select the time basis for the data to be used. Time basis is related to the available instrumentation but should be chosen depending on the purpose of the work. In addition, the time basis of the different variables involved must be similar; for example, we do not recommend the use of daily UV doses combined with one instantaneous cloud cover observation per day.

[104] 2. For a proper description of the yearly cycle and for having a large enough number of samples, databases should be at least 1 year long. Some limitation regarding SZA must be set in order to avoid poor cosine responses of measurement devices. In addition, rapidly changing sky conditions should be filtered out from the analyses. Accurate UV instrument maintenance and calibration, as well as suitable comparison of the cloudless model with cloudless measurements, should be guaranteed. Works including data and observations for different climates should be promoted. A description of cloud climatology at the measurement site should be included in the work.

[105] 3. Once the analysis has set a "cloudy model," i.e., a technique to estimate UV radiation for any sky condition, some statistical parameter regarding the accuracy of the model must be provided. In this sense, *Willmott* [1982] presented an interesting discussion about several indices for evaluating performance of model estimates. A measurement of the accuracy should be provided at least for the database used to develop the model. It is better, however, to test portability and to validate the model by using some independent database.

[106] 4. Some analyses that have already been carried out by some of the reviewed studies should be continued and eventually performed in more detail. For example, cloud effects depending on cloud type, spectral dependence of cloud effects, SZA dependence of cloud effects, and cloud enhancement effect are some issues that still have great potential for researchers.

[107] **ACKNOWLEDGMENTS.** This paper has been written within the framework of projects IMMPACTE (financed by the Department of Environment and Housing of the Catalan Government) and DEPRUVISE (financed by the Ministry of Science and Technology of the Spanish Government). We are indebted to the former Editor-in-Chief Thomas Torgersen and to the former Editor Kendall McGuffie for encouraging us to write this review and for their suggestions that allowed us to significantly improve the first draft of the manuscript. Also, the three anonymous reviewers have helped with their comments.

[108] Kendall McGuffie was the Editor responsible for this paper. He thanks two anonymous technical reviewers and one anonymous cross-disciplinary reviewer.

REFERENCES

Bais, A. F., C. S. Zerefos, C. Meleti, I. C. Ziomas, and K. Tourpali (1993), Spectral measurements of solar UVB radiation and its

relations to total ozone, SO_2 and clouds, *J. Geophys. Res.*, *98*(D3), 5199–5204.

Bais, A. F., C. S. Zerefos, and C. T. McElroy (1996), Solar UVB measurements with the double- and single-monochromator Brewer Ozone Spectrophotometers, *Geophys. Res. Lett.*, *23*(8), 833–836.

Bener, P. (1964), Investigation on the influence of clouds on the ultraviolet sky radiation, *Tech. Note 3*, Phys. Meteorol. Obs., Davos, Switzerland.

Bener, P. (1972), Approximate values of intensity of natural radiation for different amounts of atmospheric ozone, *Final Tech. Rep. DAJA 37-68-C-1017*, Eur. Res. Off., U.S. Army, London, U. K.

Berger, D. S. (1976), The sunburning ultraviolet meter: Design and performance, *Photochem. Photobiol.*, *24*, 587–593.

Bernhard, G., B. Mayer, and G. Seckmeyer (1997), Measurements of spectral solar UV irradiance in tropical Australia, *J. Geophys. Res.*, *102*(D7), 8719–8730.

Bird, R. E., and C. Riordan (1986), Simple solar spectral model for direct and diffuse irradiance on horizontal and tilted planes at the Earth's surface for cloudless atmospheres, *J. Clim. Appl. Meteorol.*, *25*, 87–97.

Blumthaler, M. (1993), UV-radiation and ozone depletion, in *Environmental Effects of Ultraviolet Radiation*, edited by M. Tevini, pp. 79–94, Lewis, Boca Raton, Fla.

Blumthaler, M., W. Ambach, and W. Rehwald (1992), Solar UV-A and UV-B radiation fluxes at two alpine stations at different altitudes, *Theor. Appl. Climatol.*, *46*, 39–44.

Blumthaler, M., A. R. Webb, G. Seckmeyer, A. F. Bais, M. Huber, and B. Mayer (1994a), Simultaneous spectroradiometry: A study of solar UV irradiance at two altitudes, *Geophys. Res. Lett.*, *21*(25), 2805–2808.

Blumthaler, M., W. Ambach, and M. Salzberg (1994b), Effects of cloudiness on global and diffuse UV irradiance in a high-mountain area, *Theor. Appl. Climatol.*, *50*, 23–30.

Bodeker, G. E., and R. L. McKenzie (1996), An algorithm for inferring surface UV irradiance including cloud effects, *J. Appl. Meteorol.*, *35*, 1860–1877.

Bordewijk, J. A., H. Slaper, H. A. J. M. Reinen, and E. Schlamann (1995), Total solar radiation and the influence of clouds and aerosols on the biologically effective UV, *Geophys. Res. Lett.*, *22*(16), 2151–2154.

Bothwell, M. L., D. M. Sherdot, and C. M. Pollock (1994), Ecosystem response to solar ultraviolet-B radiation: Influence of trophic-level interaction, *Science*, *265*, 97–100.

Bovensmann, H., S. Nöel, A. Richter, A. Rozanov, M. von König, C. V. Savigny, and J. P. Burrows (2003), SCIAMACHY on ENVISAT: Some highlights from the first year in orbit, *IGACtivities Newsl.*, *28*, 14–19.

Brasseur, A.-L., R. Ramaroson, A. Delannoy, W. Skamarock, and M. Barth (2002), Three-dimensional calculation of photolysis frequencies in the presence of clouds and impact on photochemistry, *J. Atmos. Chem.*, *41*, 211–237.

Brühl, C., and P. J. Crutzen (1989), On the disproportionate role of tropospheric ozone as a filter against solar UV-B radiation, *Geophys. Res. Lett.*, *16*(7), 703–706.

Bruls, W. A. G., H. Slaper, J. C. Van der Leun, and L. Berrens (1984), Transmission of human epidermis and stratum corneum as a function of thickness in the ultraviolet and visible wavelengths, *Photochem. Photobiol.*, *40*, 485–494.

Bryant, E. (1997), *Climate Process and Change*, 209 pp., Cambridge Univ. Press, New York.

Burkowski, J., A.-T. Chai, T. Mo, and A. E. O. Green (1977), Cloud effects on middle ultraviolet global radiation, *Acta Geophys. Pol.*, *XXV*(4), 287–301.

Burrows, W. R. (1997), CART regression models for predicting UV radiation at the ground in the presence of cloud and other environmental factors, *J. Appl. Meteorol.*, *36*, 531–544.

Buttner, K. (1938), *Physikalische Bioklimatologie: Problemen und Methoden*, *Probl. Kosmischen Phys.*, vol. 18, 155 pp., Academische, Leipzig, Germany.

Commission Internationale de l'Eclairage (CIE) (1999), 134/1, TC 6–26 Report: Standardization of the terms UV-A1, UV-A2 and UV-B, in *Collection in Photobiology and Photochemistry*, Comm. Int. de l'Eclairage, Vienna.

D'Almeida, G. A., P. Koepke, and E. P. Shettle (1991), *Studies in Geophysical Optics and Remote Sensing*, 561 pp., A. Deepak, Hampton, Va.

Diffey, B. L. (1992), Stratospheric ozone depletion and the risk of non-melanoma skin cancer in the British population, *Phys. Med. Biol.*, *37*(12), 2267–2274.

Erlick, C., and J. E. Frederick (1998), Effects of aerosols on the wavelength dependence of atmospheric transmission in the ultraviolet and visible: 2. Continental and urban aerosols in clear skies, *J. Geophys. Res.*, *103*(D18), 23,275–23,285.

Estupiñán, J. G., S. Raman, G. H. Crescenti, J. J. Streicher, and W. F. Barnard (1996), Effects of clouds and haze on UV-B radiation, *J. Geophys. Res.*, *101*(D11), 16,807–16,816.

Feister, U., and K. Gericke (1998), Cloud flagging of UV spectral irradiance measurements, *Atmos. Res.*, *49*, 115–138.

Forster, P. M. de F. (1995), Modeling ultraviolet radiation at the Earth's surface. Part I: The sensitivity of ultraviolet irradiances to atmospheric changes, *J. Appl. Meteorol.*, *34*, 2412–2425.

Foyo-Moreno, I., J. Vida, and L. Alados-Arboledas (1999), A simple all weather model to estimate ultraviolet solar radiation (290–385 nm), *J. Appl. Meteorol.*, *38*, 1020–1026.

Frederick, J. E., and H. E. Snell (1990), Tropospheric influence on solar ultraviolet radiation: The role of clouds, *J. Clim.*, *3*, 373–381.

Frederick, J. E., and H. D. Steele (1995), The transmission of sunlight through cloudy skies: An analysis based on standard meteorological information, *J. Appl. Meteorol.*, *34*, 2755–2761.

Frederick, J. E., H. E. Snell, and E. K. Haywood (1989), Solar ultraviolet radiation at the Earth's surface, *Photochem. Photobiol.*, *50*, 443–450.

Frederick, J. E., A. E. Koob, A. D. Alberts, and E. C. Weatherhead (1993), Empirical studies of tropospheric transmission in the ultraviolet: Broadband measurements, *J. Appl. Meteorol.*, *32*, 1883–1892.

Grant, R. H., and W. Gao (2003), Diffuse fraction of UV radiation under partly cloudy skies as defined by the Automated Surface Observation System (ASOS), *J. Geophys. Res.*, *108*(D2), 4046, doi:10.1029/2002JD002201.

Grant, R. H., and G. M. Heisler (2000), Estimation of ultraviolet-B irradiance under variable cloud conditions, *J. Appl. Meteorol*, *39*, 904–916.

Hader, D. P. (2000), Effects of solar UV-B radiation on aquatic ecosystems, *Adv. Space Res.*, *26*(12), 2029–2040.

Herman, J. R., P. K. Barthia, J. Ziemke, Z. Ahmad, and D. Larko (1996), UV-B increases (1979–1992) from decreases in total ozone, *Geophys. Res. Lett.*, *23*(16), 2117–2120.

Herman, J. R., N. Krotkov, E. Celarier, D. Larko, and G. Labow (1999), Distribution of UV radiation at the Earth's surface from TOMS-measured UV-backscattered radiances, *J. Geophys. Res.*, *104*(D10), 12,059–12,076.

Hess, M., P. Koepke, and I. Schult (1998), Optical properties of aerosols and clouds: The software package OPAC, *Bull. Am. Meteorol. Soc.*, *79*, 831–844.

Ilyas, M. (1987), Effect of cloudiness on solar ultraviolet radiation reaching the surface, *Atmos. Environ.*, *21*(6), 1483–1484.

Intergovernmental Panel on Climate Change (2001), *Climate Change 2001: The Scientific Basis: Contribution of Working Group I to the Third Assessment Report of the Intergovernmental Panel on Climate Change*, edited by J. T. Houghton et al., 881 pp., Cambridge Univ. Press, New York.

International Agency for Research on Cancer (1992), *Solar and Ultraviolet Radiation*, *Monogr. Eval. Carcinogenic Risks Hum.*, vol. 55, 336 pp., Geneva, Switzerland.

International Programme on Chemical Safety (IPCS) (1994), *Ultraviolet Radiation*, *Environmental Criteria*, vol. 160, World Health Organ., Geneva, Switzerland.

Iqbal, M. (1983), *An Introduction to Solar Radiation*, 101 pp., Elsevier, New York.

Janach, W. E. (1989), Surface ozone: Trend details, seasonal variations, and interpretation, *J. Geophys. Res.*, *94*(D15), 18,289–18,295.

Johnson, F. S., T. Mo, and A. E. S. Green (1976), Average latitudinal variation in ultraviolet radiation at the Earth's surface, *Photochem. Photobiol.*, *23*, 179–188.

Josefsson, W. (1986), Solar ultraviolet radiation in Sweden, *SMHI Rep. Meteorol. Climatol. 53*, 71 pp., Swed. Meteorol. and Hydrol. Inst., Norrköping, Sweden.

Josefsson, W., and T. Landelius (2000), Effect of clouds on UV irradiance: As estimated from cloud amount, cloud type, precipitation, global radiation and sunshine duration, *J. Geophys. Res.*, *105*(D4), 4927–4935.

Kalliskota, S., J. Kaurola, P. Taalas, J. R. Herman, E. A. Celarier, and A. Krotkov (2000), Comparison of daily UV doses estimated from Nimbus 7/TOMS measurements and ground-based spectroradiometric data, *J. Geophys. Res.*, *105*(D4), 5059–5067.

Kasten, F., and G. Czeplak (1980), Solar and terrestrial radiation dependent on the amount and type of cloud, *Sol. Energy*, *24*, 177–189.

Koepke, P., M. Hess, I. Schult, and E. P. Shettle (1997), Global aerosol data set, *Rep. 243*, Max-Planck-Inst. für Meteorol., Hamburg, Germany.

Koepke, P., et al. (1998), Comparison of models used for UV index calculations, *Photochem. Photobiol.*, *67*, 657–662.

Kondratyev, K. Y., and C. A. Varotsos (2000), *Atmospheric Ozone Variability: Implications for Climate Change*, *Human Health*, *and Ecosystems*, 617 pp., Praxis, Chichester, U.K.

Krotkov, N. A., P. K. Bhartia, J. R. Herman, V. Fioletov, and J. Kerr (1998), Satellite estimation of spectral surface UV irradiance in the presence of tropospheric aerosols: 1. Cloud-free case, *J. Geophys. Res.*, *103*(D8), 8779–8793.

Krzyscin, J. W., and S. Puchalski (1998), Aerosol impact on the surface UV radiation from the ground-based measurements taken at Belsk, Poland, 1980–1996, *J. Geophys. Res.*, *103*(D13), 16,175–16,181.

Krzyscin, J. W., and P. S. Sobolewski (2001), The surface UV-B irradiation in the Arctic: Observations at the Polish polar station, Hornsund (77°N, 15°E), 1996–1997, *J. Atmos. Sol. Terr. Phys.*, *63*, 321–329.

Krzyscin, J. W., J. Jaroslawski, and P. S. Sobolewski (2003), Effects of clouds on the surface erythemal UV-B irradiance at northern midlatitudes: Estimation from the observations taken at Belsk, Poland (1999–2001), *J. Atmos. Sol. Terr. Phys.*, *65*(4), 457–467.

Kuchinke, C., and M. Nunez (1999), Cloud transmission estimates of UV-B erythemal irradiance, *Theor. Appl. Climatol.*, *63*, 149–161.

Kylling, A., A. Albold, and G. Seckmeyer (1997), Transmittance of a cloud is wavelength-dependent in the UV-range: Physical interpretation, *Geophys. Res. Lett.*, *24*(4), 397–400.

Kylling, A., et al. (2003), Actinic flux determination from measurements of irradiance, *J. Geophys. Res.*, *108*(D16), 4506, doi:10.1029/2002JD003236.

Lean, C. L., R. C. Newland, D. A. Ende, E. L. Bokey, I. C. Smith, and C. E. Mountford (1993), Assessment of human colorectal biopsies by 1H MRS: Correlation with histopathology, *Magn. Res. Med.*, *30*(5), 525–533.

Lemus-Deschamps, L., L. Rikus, and P. Gies (1999), The operational Australian ultraviolet index forecast 1997, *Meteorol. Appl.*, *6*, 241–251.

Lenoble, J. (1993), *Atmospheric Radiative Transfer*, 532 pp., A. Deepak, Hampton, Va.

Liou, K. N. (1980), *An Introduction to Atmospheric Radiation*, *Int. Geophys. Ser.*, vol. 26, Elsevier, New York.

Liou, K. N. (1992), *Radiation and Cloud Process in the Atmosphere: Theory*, *Observation and Modeling*, 487 pp., Oxford Univ. Press, New York.

Long, C. N., and T. P. Ackerman (2000), Identification of clear skies from broadband pyranometer measurements and calculation of downwelling shortwave cloud effects, *J. Geophys. Res.*, *105*(D12), 15,609–15,626.

Long, C. S., A. J. Miller, H.-T. Lee, J. D. Wild, R. C. Przywarty, and D. Hufford (1996), Ultraviolet index forecasts issued by the National Weather Service, *Bull. Am. Meteorol. Soc.*, *77*(4), 729–748.

Lubin, D., and J. E. Frederick (1991), The ultraviolet radiation environment of the Antarctic Peninsula: The roles of ozone and cloud cover, *J. Appl. Meteorol.*, *30*, 478–493.

Lubin, D., E. H. Jensen, and H. P. Gies (1998), Global surface ultraviolet climatology from TOMS and ERBE data, *J. Geophys. Res.*, *103*(D20), 26,061–26,091.

Luccini, E., A. Cede, and R. D. Piacentini (2003), Effect of clouds on UV and total irradiance at Paradise Bay, Antarctic Peninsula, from a summer 2000 campaign, *Theor. Appl. Climatol.*, *75*, 105–116.

Madronich, S. (1993), UV radiation in the natural and perturbed atmosphere, in *Environmental Effects of Ultraviolet Radiation*, edited by M. Tevini, pp. 17–69, Lewis, Boca Raton, Fla.

Matthijsen, J., H. Slaper, H. A. J. M. Reinen, and G. J. M. Velders (2000), Reduction of solar UV by clouds: A comparison between satellite-derived cloud effects and ground-based radiation measurements, *J. Geophys. Res.*, *105*(D4), 5069–5080.

Mayer, B., G. Seckmeyer, and A. Kylling (1997), Systematic long-term comparison of spectral UV measurements and UVSPEC modeling results, *J. Geophys. Res.*, *102*(D7), 8755–8767.

Mayer, B., A. Kylling, S. Madronich, and G. Seckmeyer (1998), Enhanced absorption of UV radiation due to multiple scattering in clouds: Experimental evidence and theoretical explanation, *J. Geophys. Res.*, *103*(D23), 31,241–31,254.

McKenzie, E. L., W. A. Matheus, and P. V. Johnson (1991), The relationship between erythemal UV and ozone, derived from spectral irradiance measurements, *Geophys. Res. Lett.*, *18*(12), 2269–2272.

McKenzie, R. L., G. E. Bodeker, D. J. Keep, M. Kotkamp, and J. M. Evans (1996), UV radiation in New Zealand: Measured north to south differences, and relationship to other latitudes, *Weather Clim.*, *16*, 17–26.

McKenzie, R. L., P. V. Johnston, D. Smile, B. A. Bodhaine, and S. Madronich (2001), Altitude effects on UV spectral radiance deduced from measurements at Lauder, New Zealand, and Mauna Loa Observatory, Hawaii, *J. Geophys. Res.*, *106*(D19), 22,845–22,860.

McKinlay, A. F., and B. L. Diffey (1987), A reference action spectrum for ultraviolet induced erythema in human skin, *CIE J.*, *6*, 17–22.

Meerkoetter, R., B. Wissinger, and G. Seckmeyer (1997), Surface UV from ERS-2/GOME and NOAA/AVHRR data: A case study, *Geophys. Res. Lett.*, *24*(15), 1939–1942.

Nann, S., and C. Riordan (1991), Solar spectral irradiance under clear and cloudy skies: Measurements and semiempirical model, *J. Appl. Meteorol.*, *30*, 447–462.

Neale, P. J., R. F. Davis, and J. J. Cullen (1998), Interactive effects of ozone depletion and vertical mixing on photosynthesis of Antarctic phytoplankton, *Nature*, *392*(6676), 585–589.

Paltridge, G. W., and I. J. Barton (1978), Erythemal ultraviolet radiation distribution over Australia–The calculations, detailed results and input data, *Tech. Pap. 33*, 48 pp., Aust. Div. of Atmos. Phys., Commonw. Sci. and Indus. Res. Organ., Aspendale, Victoria, Australia.

Parisi, A. V., J. Sabburg, and M. G. Kimlin (2004), *Scattered and Filtered Solar UV Measurements*, *Adv. Global Change Res.*, vol. 17, 195 pp., Springer, New York.

Piazena, H. (1996), The effect of altitude upon the solar UV-B and UV-A irradiance in the tropical Chilean Andes, *Sol. Energy*, *57*, 133–140.

Prézelin, B. B., N. P. Boucher, and O. Schofield (1994), Evaluation of field studies of UVB radiation effects on Antarctic marine

primary productivity, in *Stratospheric Ozone Depletion Depletion/UV-B Radiation in the Biosphere*, *NATO ASI Ser.*, *Ser. I*, vol. 18, edited by H. Biggs and M. E. B. Joyner, pp. 181–194, Springer, New York.

Renaud, A., J. Staehelin, C. Fröhlich, R. Philipona, and A. Heimo (2000), Influence of snow and clouds on erythemal UV radiation: Analysis of Swiss measurements and comparison with models, *J. Geophys. Res.*, *105*(D4), 4961–4969.

Repacholi, M. H. (2000), Global solar UV index, *Radiat. Prot. Dosim.*, *91*(1–3), 307–315.

Sabburg, J., and J. Wong (2000a), The effect of clouds on enhancing UVB irradiance at the Earth's surface: A one year study, *Geophys. Res. Lett.*, *27*(20), 3337–3340.

Sabburg, J., and J. Wong (2000b), Evaluation of sky/cloud formula for estimating UV-B irradiance under cloudy skies, *J. Geophys. Res.*, *105*(D24), 29,685–29,691.

Sabburg, J. M., A. V. Parisi, and M. G. Kimlin (2003), Enhanced spectral UV irradiance: A 1 year preliminary study, *Atmos. Res.*, *66*(4), 261–272.

Schafer, J. S., V. K. Saxena, B. N. Wenny, W. Barnard, and J. J. DeLuisi (1996), Observed influences of clouds on ultraviolet-B radiation, *Geophys. Res. Lett.*, *23*(19), 2625–2628.

Schippnick, P. F., and A. E. S. Green (1982), Analytical characterization of spectral irradiance in the middle ultraviolet, *Photochem. Photobiol.*, *35*, 89–101.

Schwander, H., P. Koepke, and A. Ruggaber (1997), Uncertainties in modeled UV irradiances due to limited accuracy and availability of input data, *J. Geophys. Res.*, *102*(D8), 9414–9429.

Schwander, H., P. Koepke, A. Kaifel, and G. Seckmeyer (2002), Modification of spectral UV irradiance by clouds, *J. Geophys. Res.*, *107*(D16), 4296, doi:10.1029/2001JD001297.

Seckmeyer, G. (2000), Coordinated ultraviolet radiation measurements, *Radiat. Prot. Dosim.*, *91*(1–3), 99–103.

Seckmeyer, G., R. Erb, and A. Albold (1996), Transmittance of a cloud is wavelength-dependent in the UV-range, *Geophys. Res. Lett.*, *23*(20), 2753–2755.

Seinfeld, J. H., and S. N. Pandis (1997), *Atmospheric Chemistry and Physics*, *From Air Pollution to Climate Change*, 1326 pp., John Wiley, Hoboken, N. J.

Selgrade, M. J., M. H. Repacholi, and H. S. Koren (1997), Ultraviolet radiation-induced immune modulation: Protection consequences for infections, allergic and autoimmune disease, *Environ. Health Perspect.*, *105*(3), 332–334.

Setlow, B. (1974), The wavelength in sunlight effective in producing skin cancer: A theoretical analysis, *Proc. Natl. Acad. Sci. U. S. A.*, *71*(9), 3363–3366.

Setlow, R. B., E. Grist, K. Thompson, and A. D. Woodhead (1993), Wavelengths effective in induction of malignant melanoma, *Proc. Natl. Acad. Sci. U. S. A.*, *90*(14), 6666–6670.

Sinha, R. P., and D. P. Hader (2002), Life under solar UV radiation in aquatic organisms, *Adv. Space Res.*, *30*(6), 1547–1556.

Smith, R. C., et al. (1992), Ozone depletion: Ultraviolet radiation and phytoplankton biology in Antarctic waters, *Science*, *255*(5047), 952–959.

Thiel, S., K. Steiner, and H. K. Seidlitz (1997), Modification of global erythemally effective irradiance by clouds, *Photochem. Photobiol.*, *65*, 969–973.

Thomas, G. E., and K. Stamnes (1999), *Radiative Transfer in the Atmosphere and Ocean*, 517 pp., Cambridge Univ. Press, New York.

Trepte, S., and P. Winkler (2004), Reconstruction of erythemal UV irradiance and dose at Hohenpeissenberg (1968–2001) considering trends of total ozone, cloudiness and turbidity, *Theor. Appl. Climatol*, *77*, 159–171.

Vanicek, K., T. Frei, Z. Litynska, and A. Schmalwieser (2000), UV-index for the public: A guide for publication and interpretation of solar UV index forecasts for the public prepared by the Working Group 4 of the COST-713 action "UVB forecasting," report, 26 pp., Eur. Coop. in the Field of Sci. and Tech. Res., Brussels.

Van Weele, M. (1996), Effect of clouds on ultraviolet radiation: Photodissociation rates of chemical species in the troposphere, Ph.D. thesis, Univ. of Utrecht, Utrecht, Netherlands.

Van Weele, M., et al. (2000), From model intercomparison toward benchmark UV spectra for six real atmospheric cases, *J. Geophys. Res.*, *105*(D4), 4915–4925.

Weatherhead, E. C., G. C. Tiao, G. C. Reinsel, J. E. Frederick, J. J. DeLuisi, D. S. Choi, and W. K. Tam (1997), Analysis of long-term behavior of ultraviolet radiation measured by Robertson-Berger meters at 14 sites in the United States, *J. Geophys. Res.*, *102*(D7), 8737–8754.

Webb, A. R. (1998), *UVB Instrumentation and Applications*, Gordon and Breach, New York.

Webb, A. R. (2000), Standardisation of data from ultraviolet radiation detectors, *Radiat. Protect. Dosim.*, *91*(1–3), 123–128.

Webb, A. R., R. Kift, S. Thiel, and M. Blumthaler (2002), An empirical method for the conversion of spectral UV irradiance measurements to actinic flux data, *Atmos. Environ.*, *36*, 4397–4404.

Weihs, P., and A. R. Webb (1997), Accuracy of spectral UV model calculations: 1. Consideration of uncertainties in input parameters, *J. Geophys. Res.*, *102*(D1), 1541–1550.

Weihs, P., G. Rengarajan, S. Simic, W. Laube, and W. Mikielewicz (2000), Measurements of the reflectivity in the ultraviolet and visible wavelength range in a mountainous region, *Radiat. Prot. Dosim.*, *91*(1–3), 193–195.

World Health Organization (WHO) (1995), Protection against exposure to ultraviolet radiation, *Rep. WHO/EHG/95.17*, Geneva, Switzerland.

Willmott, C. J. (1982), Some comments on the evaluation of model performance, *Bull. Am. Meteorol. Soc.*, *63*, 1309–1313.

World Health Organization (WHO) (2002), Global solar UV index: A practical guide, report, 26 pp., Geneva, Switzerland.

Williams, J. E., P. N. den Outer, H. Slaper, J. Matthijsen, and G. Kepflens (2004), Cloud induced reduction of solar UV-radiation: A comparison of ground-based and satellite based approaches, *Geophys. Res. Lett.*, *31*, L03104, doi:10.1029/2003GL018242.

World Meteorological Organization (1994a), Scientific assessment of ozone depletion: 1994, *Global Ozone Res. Monit. Proj. Rep. 37*, Geneva, Switzerland.

World Meteorological Organization (1994b), Report of the WMO meeting of experts on UV-B measurements, data, quality and standardization of UV indices, *WMO Rep. 95*, Les Diablerets, Switzerland.

World Meteorological Organization (1999), Scientific assessment of ozone depletion: 1998, *Global Ozone Res. Monit. Proj. Rep. 44*, Geneva, Switzerland.

World Meteorological Organization (2003), Scientific assessment of ozone depletion: 2002, *Global Ozone Res. Monit. Proj. Rep. 47*, 498 pp., Geneva, Switzerland.

Ziemke, J. R., J. R. Herman, J. L. Stanford, and P. K. Bhartia (1998), Total ozone/UVB monitoring and forecasting: Impact of clouds and the horizontal resolution of satellite retrievals, *J. Geophys. Res.*, *103*(D4), 3865–3871.

Ziemke, J., S. Chandra, J. Herman, and C. Varotsos (2000), Erythemal weighted UV trends over northern latitudes derived from Nimbus 7 TOMS measurements, *J. Geophys. Res.*, *105*(D6), 7373–7382.

J. Calbó, J.-A. González, and D. Pagès, Departament de Física, Universitat de Girona, Campus Montilivi, EPS-II, 17071 Girona, Spain. (josep.calbo@udg.es)